Cell Reports

Article

Comparing the Effects of Low-Protein and High-Carbohydrate Diets and Caloric Restriction on Brain Aging in Mice

Graphical Abstract

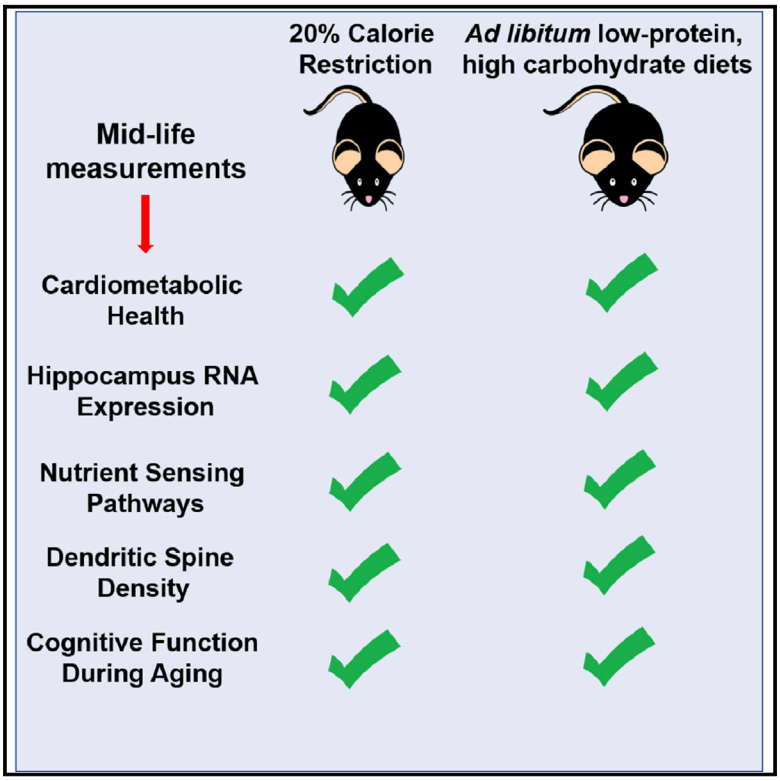

Highlights

- Calorie restriction (CR) and low-protein, high-carb (LPHC) diets improve health
- Hippocampus RNA expression is positively influenced by CR and LPHC diets
- Nutrient-sensing pathways are similarly influenced by CR and LPHC diets
- CR and LPHC diets positively influence dendritic spines and cognitive function

Authors

Devin Wahl, Samantha M. Solon-Biet, Qiao-Ping Wang, ..., Victoria C. Cogger, Stephen J. Simpson, David G. Le Couteur

Correspondence

stephen.simpson@sydney.edu.au (S.J.S.), david.lecouteur@sydney.edu.au (D.G.L.C.)

In Brief

Calorie restriction (CR) and *ad libitum* low-protein, high-carbohydrate (LPHC) diets improve cardiometabolic health in mice. Wahl et al. show that, like healthspan, CR and LPHC diets positively affect hippocampus biology in mice by influencing hippocampus gene expression, nutrient-sensing pathways, dendritic morphology, and cognition.

Wahl et al., 2018, Cell Reports *25*, 2234–2243
November 20, 2018
https://doi.org/10.1016/j.celrep.2018.10.070

CellPress

OPEN ACCESS
CellPress

Cell Reports
Article

Comparing the Effects of Low-Protein and High-Carbohydrate Diets and Caloric Restriction on Brain Aging in Mice

Devin Wahl,[1,2] Samantha M. Solon-Biet,[1] Qiao-Ping Wang,[1,3] Jibran A. Wali,[1] Tamara Pulpitel,[1] Ximonie Clark,[1] David Raubenheimer,[1] Alistair M. Senior,[1,4] David A. Sinclair,[5,6] Gregory J. Cooney,[1] Rafael de Cabo,[7] Victoria C. Cogger,[1,2] Stephen J. Simpson,[1,*] and David G. Le Couteur[1,2,8,*]

[1]Charles Perkins Centre, The University of Sydney, Sydney, NSW 2006, Australia
[2]Aging and Alzheimers Institute, ANZAC Research Institute, Centre for Education and Research on Ageing, Concord, NSW 2139, Australia
[3]School of Pharmaceutical Sciences (Shenzhen), Sun Yat-sen University, Guangzhou 510275, China
[4]School of Mathematics and Statistics, The University of Sydney, NSW 2006, Australia
[5]Department of Genetics, Paul F. Glenn Center for the Biology of Aging, Harvard Medical School, Boston, MA 02115, USA
[6]Department of Pharmacology, School of Medical Sciences, The University of New South Wales, Sydney, NSW 2052, Australia
[7]Translational Gerontology Branch, National Institute on Aging, NIH, Baltimore, MD 21224, USA
[8]Lead Contact
*Correspondence: stephen.simpson@sydney.edu.au (S.J.S.), david.lecouteur@sydney.edu.au (D.G.L.C.)
https://doi.org/10.1016/j.celrep.2018.10.070

SUMMARY

Calorie restriction (CR) increases lifespan and improves brain health in mice. *Ad libitum* low-protein, high-carbohydrate (LPHC) diets also extend lifespan, but it is not known whether they are beneficial for brain health. We compared hippocampus biology and memory in mice subjected to 20% CR or provided *ad libitum* access to one of three LPHC diets or to a control diet. Patterns of RNA expression in the hippocampus of 15-month-old mice were similar between mice fed CR and LPHC diets when we looked at genes associated with longevity, cytokines, and dendrite morphogenesis. Nutrient-sensing proteins, including SIRT1, mTOR, and PGC1α, were also influenced by diet; however, the effects varied by sex. CR and LPHC diets were associated with increased dendritic spines in dentate gyrus neurons. Mice fed CR and LPHC diets had modest improvements in the Barnes maze and novel object recognition. LPHC diets recapitulate some of the benefits of CR on brain aging.

INTRODUCTION

Nutritional interventions, such as caloric restriction (CR), influence aging and age-related changes in the brain (Mattson et al., 2018; Wahl et al., 2016). CR improves cognitive function, including learning and memory, in old rodents (Ingram et al., 1987; Wahl et al., 2017), possibly mediated by its effects on cardiometabolic risk factors, generic hallmarks of aging, specific brain-related mechanisms (BDNF, neurogenesis) or nutrient-sensing pathways (Wahl et al., 2016).

CR is not readily translatable in humans. Therefore, other interventions that recapitulate the benefits of CR on brain function without the requirement for long-term reduction in food intake are being explored. Recently, we utilized the geometric framework (Simpson and Raubenheimer, 2012) to evaluate the effects of *ad libitum*-fed diets varying in macronutrients and energy content on aging. Mice consuming a low-protein, high-carbohydrate, low-fat diet (LPHC, protein:carbohydrate ~1:10) lived longest and were healthier in old age, even when compared to CR achieved by dilution of chow with non-digestible fiber (Solon-Biet et al., 2014). The beneficial effects of LPHC diets on lifespan are conserved across a range of organisms from invertebrates to mice (Le Couteur et al., 2016).

The effects of LPHC diets on brain aging are unknown. However, the observation that *ad libitum*-fed LPHC diets are beneficial for lifespan and late-in-life cardiometabolic health suggest that they may also delay brain aging. To test this hypothesis, we evaluated the effects of four *ad-libitum*-fed diets varying in protein and carbohydrates and compared them to a standard 20% CR regimen in mice. Metabolic phenotype and markers of cognitive function and underlying neurobiological processes were investigated with a focus on the hippocampus. Despite differences in aspects of metabolic phenotype, *ad libitum* LPHC diets conferred benefits to the hippocampus that are similar to standard 20% CR.

RESULTS

Cardiometabolic Parameters and Body Composition

Systemic parameters were determined at 15 months of age in mice fed one of five diets from weaning; diets are shown in Table 1. Daily energy intake, which rose with dilution of dietary protein by carbohydrate, was maximal on the 5% protein diet (Figures 1A and 1B), consistent with protein leverage (Sørensen et al., 2008). Overall, CR and/or 5% protein diets were associated with lower body fat and weight, glucose tolerance, insulin, and leptin and higher adiponectin and FGF-21 (Figures 1C and 1K). These diets had no significant effect on insulin-like growth factor 1 (IGF-1) (Figure 1I), whereas cholesterol was highest on the 10% protein diet and lowest with CR (Figure 1L). There were some differences between male and female mice as

Table 1. Diets Used in the Study

Diet	NME (kJ/g)	% Protein NME	% Carbohydrate NME	% Fat NME
CR	14.4	18.8	63.4	17.8
5% protein	14.4	5	77.2	17.8
10% protein	14.4	10	72.2	17.8
15% protein	14.4	15	67.2	17.8
19% protein	14.4	18.8	63.4	17.8

CR, calorie restriction; NME, net metabolizable energy.

shown. Other differences found included: urea, albumin, alanine transaminase and the exchange ratio of CO_2 and O_2 (respiratory quotient, RQ) (Table S1).

Hippocampal Gene Expression

Hierarchical clustering of differentially expressed genes from total hippocampus tissue revealed differences between the dietary groups as visualized with a heatmap (Figure 2A). Principle component analysis did not reveal differences between sexes (data not shown) and were therefore combined. CR had a marked effect on gene expression compared to control diet, while LPHC diets were associated with intermediate patterns of expression. The top-10 differentially expressed genes are listed in Table S2. Protein-Coupled Receptor 17 (*Gpr17*) is the top upregulated gene for all LPHC diets. CR was associated with altered expression of genes associated with circadian rhythm (*Dbp*) (Nikonova et al., 2017) and neuronal proliferation (*Dchs1*) (Beste et al., 2016).

FPKM (fragments per kilobase of transcript per million mapped reads) values were used to construct a volcano plot for gene expression that correlated with protein intake (Figure 2B; Table S3). The top gene positively correlated with protein intake was Gamma-aminobutyric acid type A receptor beta 2 subunit (*Gabrb2)*, that encodes $GABA_A$ receptors. The top gene negatively correlated with protein intake was Zinc-Finger CCCH-Type-Containing 13 (*Zc3h13*), which is involved in nuclear factor κB (NF-κB) production (Gewurz et al., 2012).

Overlap of genes influenced by CR or correlated with protein intake was determined (Figure 2C). Compared to expression with control diet, CR was associated with 237 genes that were upregulated and 238 genes that were downregulated. There were 379 genes that were upregulated with lower protein (and higher carbohydrate) intake and 438 genes that were downregulated with lower protein (and higher carbohydrate) intake. Only 40 overexpressed genes and 34 underexpressed genes were shared between CR and lower protein intake (Table S4), and several of these were of interest, including Semaphorin 4B (*Sema4b*), which is involved in synapse formation (Paradis et al., 2007), and Carboxypeptidase E (*Cpe*), which is a trophic factor that might influence neuron survival during aging (Cheng et al., 2014).

The effects of diets on biological pathways were determined (Figure 2D; Table S5). Pathways influenced by diet included several brain-specific and general cellular processes; surprisingly few overlapping pathways were among the groups. However, dendrite morphogenesis, synapse functioning, and neuronal development pathways were influenced by CR and dietary protein.

The changes in gene expression induced by the different diets were compared to genes that are reported to influence aging in mice (GenAge: The Aging Gene Database [http://genomics.senescence.info/genes/]) (Figures 2E and 2F; Tables S6 and S7). The patterns of expression (determined by log2fold change compared with 19% protein diet) with LPHC and CR diets were similar when categorized by genes that shorten lifespan ("Anti-longevity" genes) and those that extend lifespan ("pro-longevity" genes). CR and LPHC diets upregulated and downregulated both anti-longevity and pro-longevity genes in variable patterns.

Hippocampal Nutrient-Sensing Pathway Proteins

CR elicits beneficial responses in the hippocampus via expression of nutrient-sensing proteins (Pani, 2015), including SIRT1, PGC1α, and MTOR. We found significant sex differences in the hippocampal expression of these proteins. In female mice SIRT1 protein expression was greatest in CR and 5% protein diets while in male mice there were no effect of diet (Figure 3A). In female mice MTOR activation (p-MTOR/MTOR) was lowest with CR and lowest protein diets (Figure 3B) and there was a positive correlation with MTOR activation and protein intake (and a negative correlation with carbohydrate intake) in both male and female mice (Figure S2A). PGC1α protein expression was increased only in male mice on CR (Figure 3C).

The top genes that are consistently upregulated (Figure 3D) and downregulated (Figure 3E) with CR from a recent meta-analysis (Plank et al., 2012) were compared with their expression in this study. CR and LPHC had similar effects on the patterns of expression. Several genes of interest, including Carbonyl reductase 1 (*Cbr1*), contribute to protection against oxidative damage and ischemia (Kim et al., 2014) (Figures 3D and 3E; Table S8).

Hippocampal Markers of Neuroinflammation

Pro-inflammatory cytokines interleukin (IL)-6 and tumor necrosis factor alpha (TNF-α), the anti-inflammatory cytokine IL-10 and brain-derived neurotrophic factor (BDNF) were measured. There was an increase in hippocampus IL-10 in lowest protein and CR diets (Figure S1A) but no changes in TNF-α, IL6, or BDNF (Figures S1B, S1C, and S1F). There were no significant differences among the groups in the number of hippocampus $Iba1^+$ cells (Figure S1D and S1E). Next, we looked at total hippocampus GFAP expression as measured by immunofluorescence but were not able to detect any differences among the groups (Figure S1G; Table S9).

Changes in gene expression were compared to those reported to influence cytokine response (AmiGO online gene ontology database: http://amigo.geneontology.org/amigo) (Figure S1H; Table S9). The patterns of expression with LPHC and CR diets were similar in terms of their effect on genes influencing cytokine response. A gene of interest was Suppressor of Cytokine 1 (*Socs1*), which is involved in suppressing brain inflammation (Walker et al., 2015).

Dendritic Spine Density in the Hippocampus Dentate Gyrus

The lowest protein and CR groups had increased dendrite spine density in the dentate gyrus (Figures 4A and 4B). However, the protein expression of drebrin, which is involved in the

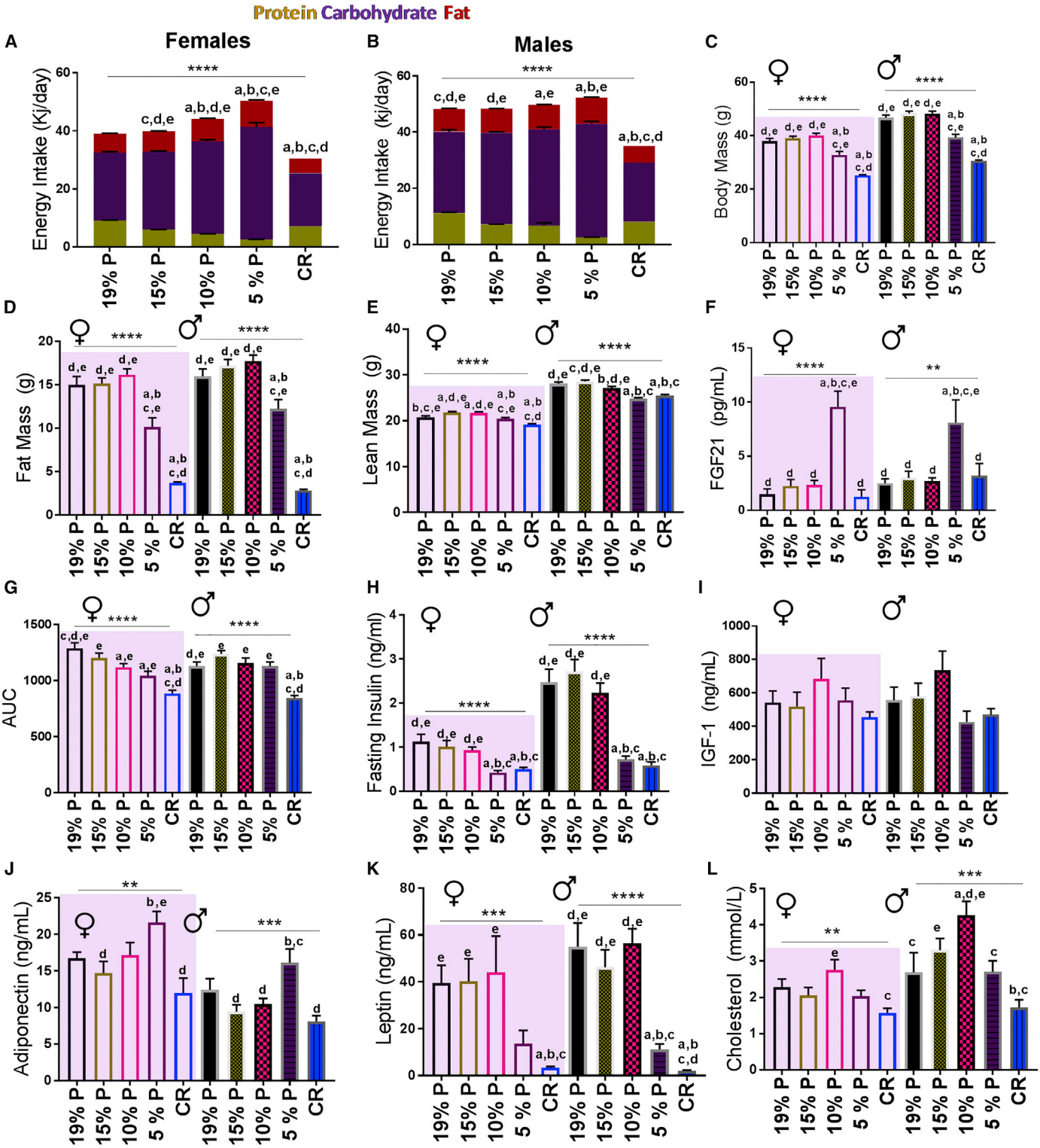

Figure 1. Impact of CR and LPHC Diets on Cardiometabolic Health in Male and Female 15-Month-Old Mice

(A) Female daily energy intake (kJ/day) by macronutrient.

(B) Male daily energy intake (kJ/day) by macronutrient.

(C) Body mass of mice. n = 25–30 mice per group.

(D) Total fat mass. n = 25–35 mice per experimental group.

(legend continued on next page)

maintenance and formation of dendritic spines, was unchanged (Figure S2B).

The changes in gene expression induced by diet were compared to genes that are reported to influence dendrite morphogenesis (AmiGO online gene ontology database: http://amigo.geneontology.org/amigo) (Figure 4C; Table S10). The patterns of expression with LPHC and CR diets showed increasing upregulation of these genes as protein content of the diet decreased and with CR.

Memory and Learning in Middle-Aged and Old Mice

The Barnes maze and novel object recognition tests were used to assess the effects of diet on memory and learning at 13 and 23 months of age. Overall, changes in some parameters tended to show a benefit for CR and lower protein diets primarily in female mice.

In 13-month-old females, CR was associated with best performance on the Barnes maze on days 1 and 2, whereas, in 23-month-old females, CR was associated with best performance on day 4. The lower protein diets were also associated with some trends suggestive of improvement, with the 15% protein diet having the best performance on day 3 in the 13-month-old female mice and the 10% protein diet having the best performance on day 3 in the 23-month-old female mice (Figures 5A and 5B). In male mice, the only significant finding was that the 13-month-old mice on 10% protein diets performed best on days 2 and 3 (Figures 5C and 5D).

The significant findings for the novel object recognition test were that the 13-month-old female mice on the CR and 10% protein diets had the best recognition indices (Figure 5E). Interestingly, there was a negative correlation with body fat at young age and subsequent old-age recognition index scores (Figure 5G).

DISCUSSION

Aging is a powerful risk factor for the development of many diseases, particularly dementia. Identifying nutritional interventions that delay brain aging and can be easily implemented in humans is especially important because no pharmacological treatments have been discovered that maintain brain function or reduce the risk of dementia. In this study, the effects of *ad libitum* LPHC diets on brain aging were studied and compared with standard CR.

Studies of CR and protein restriction on brain health and neurodegenerative disease in aging rodents have usually shown positive outcomes (Ingram et al., 1987; Mattson, 2010; Newman et al., 2017; Pani, 2015; Parrella et al., 2013). In our study, CR diets and LPHC diets were associated with modest improvements in behavioral and cognitive outcomes, although the results were mainly limited to females and inconsistent. Of note, the standard chow diet did not perform best for any measurement at any time point or for either sex. The results provide some support for the conclusion that CR and possibly LPHC diets improve brain function in old age.

CR and LPHC diets had marked effects on systemic cardiometabolic outcomes, which are increasingly recognized as risk factors for cognitive impairment and the risk of neurodegenerative disease (Buffa et al., 2014; Dye et al., 2017). These results are consistent with other studies of CR and LPHC diets (Simpson et al., 2017; Solon-Biet et al., 2015; Testa et al., 2014). FGF-21, a hormone linked with cardiometabolic health, was elevated in the 5% protein group, confirming our previous conclusion that FGF-21 is driven by low dietary protein coupled with elevated carbohydrate intake (Solon-Biet et al., 2016). Midlife body fat in females was correlated with novel object recognition in old mice, which parallels human observational studies linking midlife obesity with subsequent risk of dementia (Tolppanen et al., 2014).

We examined the effects of CR and LPHC diets on hippocampal gene expression. Other studies have reported changes in hippocampal gene expression with food restriction (Wood et al., 2015), influencing age-dependent changes in gene expression (Prolla and Mattson, 2001; Schafer et al., 2015), including genes involved with oxidative stress (Schafer et al., 2015) mitochondrial function and synaptic plasticity (Zeier et al., 2011). Overall, we found that gene expression signatures in CR and LPHC diets were different; however, there were similarities when specific genes involved with brain aging were analyzed, such as prolongevity genes, antilongevity genes, and genes involved with CR, inflammation, and dendrite morphogenesis.

The top upregulated gene for all three LPHC groups was the G-protein-coupled receptor, *Gpr17*. *Gpr17* is widely expressed in the brain, particularly in neuroprogenitor cells and contributes to myelination of axons and neuronal repair after acute injury (Alavi et al., 2018). Intriguingly *Gpr17* also has been found to be involved with food intake; knockout of *Gpr17* reduced food consumption in mice (Ren et al., 2012). Our data suggest that *Gpr17* expression responds to dietary macronutrient balance, which provides a mechanistic link between diet and brain aging.

(E) Total lean mass. n = 25–35 mice per experimental group.
(F) Serum FGF-21. n = 10–12 mice per experimental group.
(G) Glucose tolerance test (area under the curve, AUC). n = 20–30 mice per group.
(H) Fasted serum insulin. n = 20–30 mice per group.
(I) Serum IGF-1. n = 10–12 mice per group.
(J) Serum adiponectin. n = 10–12 mice per group.
(K) Serum leptin. n = 10–12 mice per group.
(L) Serum cholesterol. n = 10–12 mice per experimental group.
*p < 0.05; **p < 0.01; ***p < 0.001; ****p < 0.0001 ANOVA analysis. a = significantly different to 19% P; b = significantly different to 15% P; c = significantly different to 10% P; d = significantly different to 5% P; e = significantly different to CR as determined by a Tukey's post hoc analysis. Mean ± SEM.
See also Table S1.

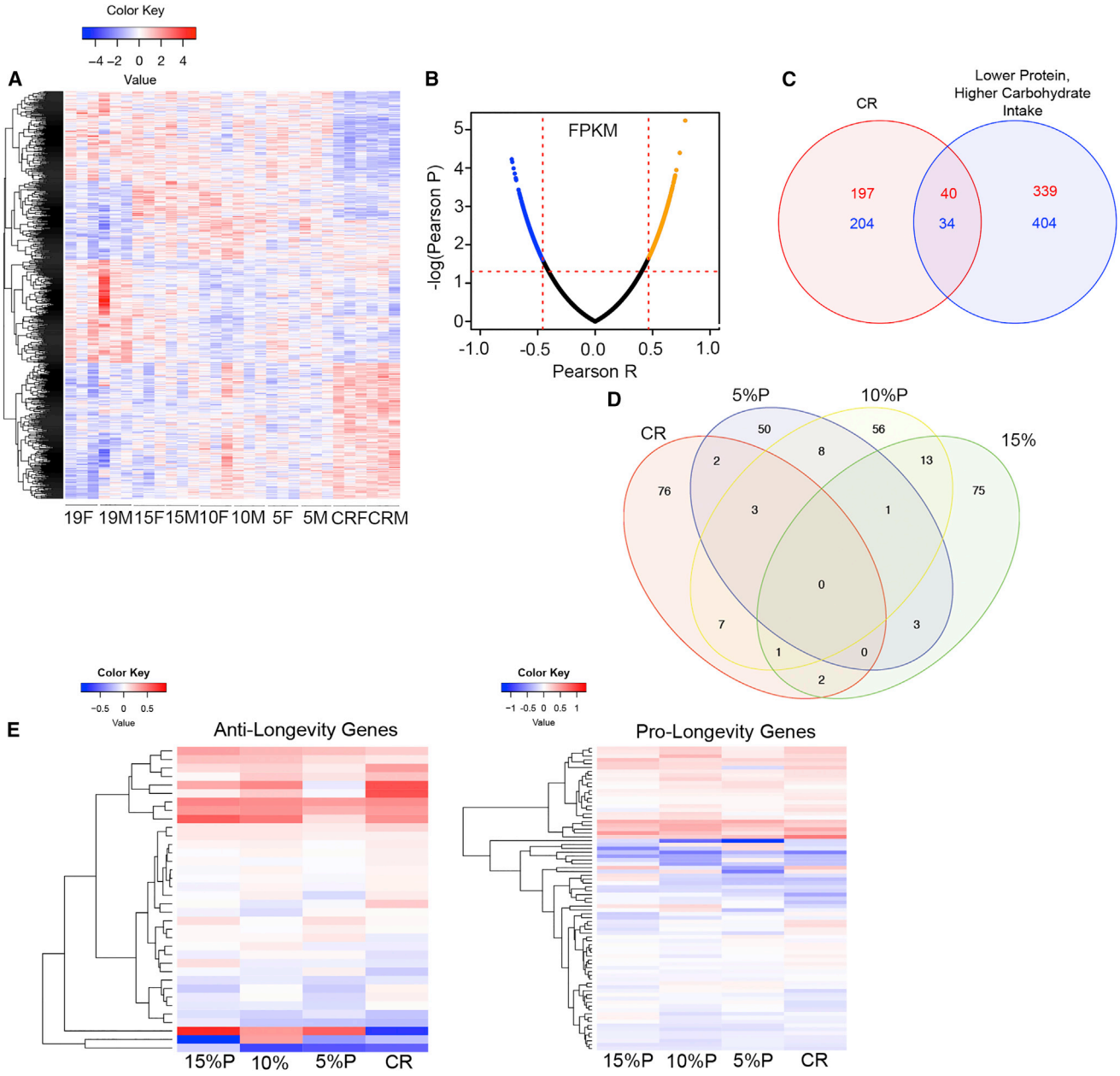

Figure 2. Impact of CR and LPHC Diets on Hippocampal Gene Expression in Male and in Female 15-Month-Old Mice

(A) Heatmap of upregulated or downregulated genes compared to average expression across all genes as measured by the row of standardized *Z* scores. n = 3 mice per experimental group.

(B) Volcano plot of the top 5% of genes positively correlated or negatively correlated with daily protein intake. n = 3 mice per experimental group.

(C) Venn diagram showing genes upregulated (red) or downregulated (blue) by CR when compared to control 19% protein diet and genes overexpressed with lower protein intake (red) and underexpressed with lower protein intake (blue) as measured by a Pearson correlation.

(D) Venn diagram of total differentiated biological processes among the groups. Each group was compared to control 19% protein diet. n = 6 biological replicates per group

(E) Heatmap of significantly upregulated or downregulated genes identified by GenAge as anti-longevity genes. Each experimental group is compared to control 19% protein diet, and the degree of relatedness among the genes is shown on the y axis. n = 6 replicates per group.

(F) Heatmap of significantly upregulated or downregulated genes identified by GenAge as pro-longevity genes. Each group is compared to control 19% protein diets, and the degree of relatedness among the genes is shown on the y axis. n = 6 replicates group.

See also Tables S2, S3, S4, S5, S6, and S7.

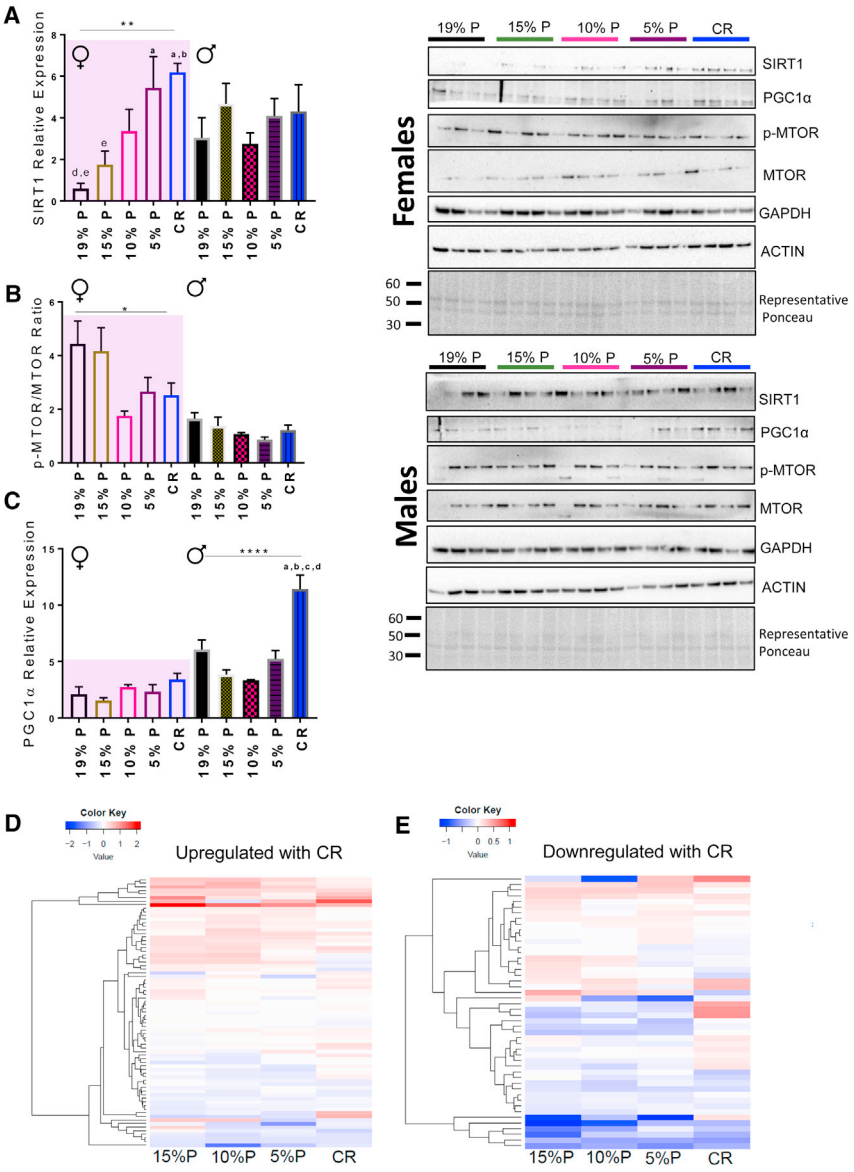

Figure 3. Changes in the Expression of Several Key Nutrient-Sensing Proteins and CR Genes in Response to CR and LPHC Diets at 15 Months of Age

(A) SIRT1 protein expression from whole hippocampus homogenates. n = 4 mice per group.

(B) The ratio of phospho-MTOR:total MTOR expression from whole-hippocampus homogenates. n = 4 mice per group. See also Figure S2.

(C) PGC1-α protein expression from whole hippocampus homogenates. n = 4 per group. Representative Ponceau S staining is shown, and each band was normalized to the total densitometric value for total protein per lane.

(D) Heatmap of genes known to be upregulated with CR. Each group was compared to control 19% protein diets, and the degree of relatedness among the genes is shown on the y axis. n = 6 replicates per group. See also Table S8.

(E) Heatmap of genes known to be downregulated with CR. Each group was compared to control 19% protein diets, and the degree of relatedness among the genes is shown on the y axis. n = 6 replicates per group. See also table S8.

*p < 0.05; **p < 0.01; ***p < 0.001; ****p < 0.0001 ANOVA analysis. a = significantly different to 19% P; b = significantly different to 15% P; c = significantly different to 10% P; d = significantly different to 5% P; e = significantly different to CR as determined by a Tukey's post hoc analysis. All data are presented by the mean ± SEM of the biological replicates.

The beneficial effects of CR on aging are in part mediated by its impact on several nutrient-sensing pathways such as SIRT1, MTOR, and PGC1α (Hadem et al., 2017), which also have been linked with brain aging (Mazucanti et al., 2015). We found that SIRT1 and MTOR were influenced by CR and dietary P:C only in female mice, while PGC1α was markedly increased in males with CR. Our results are consistent with other studies showing a sex-specific effect of CR on nutrient-sensing pathways and outcomes (Mitchell et al., 2016).

CR has been reported to reduce pro-inflammatory cytokines, increase anti-inflammatory cytokines (Willette et al., 2013) and increase BDNF in the hippocampus (Stranahan et al., 2009). We found that CR and LPHC were associated with increased levels of the anti-inflammatory cytokine IL-10, which influences brain response to acute injury (Garcia et al., 2017), while IL-10 in macrophages decreases with age and impairs recovery from neural injury (Zhang et al., 2015). We couldn't detect any effect of nutrition on other inflammatory cytokines, including IL6 and TNFα or the neurotrophic cytokine, BDNF. Increased expression of glial fibrillary acidic protein (GFAP) has been linked with inflammation, astroglial activation, and gliosis during brain degeneration (Brahmachari et al., 2006). Therefore, we investigated the effects of the nutritional interventions on total GFAP immunofluorescence expression in the hippocampus. We were not able to detect any changes among the groups in GFAP expression, suggesting that the dietary interventions in the current study did not influence neuroinflammatory processes that have been associated with neurodegenerative disease.

The dentate gyrus (DG) of the hippocampus contributes to the consolidation and formation of spatial memory, and dendritic spines in the DG are important for optimal neuronal function and the formation of memories (Kesner, 2017). CR has been reported to increase DG dendritic spine density in a mouse model of diabetes (Stranahan et al., 2009). We found that both CR and 5% protein diets increased dendritic spine density, consistent with the role of dendritic spines in cognitive and behavioral outcomes and the response to dietary interventions.

We recognize limitations to the current study. First, analyses of the hippocampus and metabolic data were acquired at only

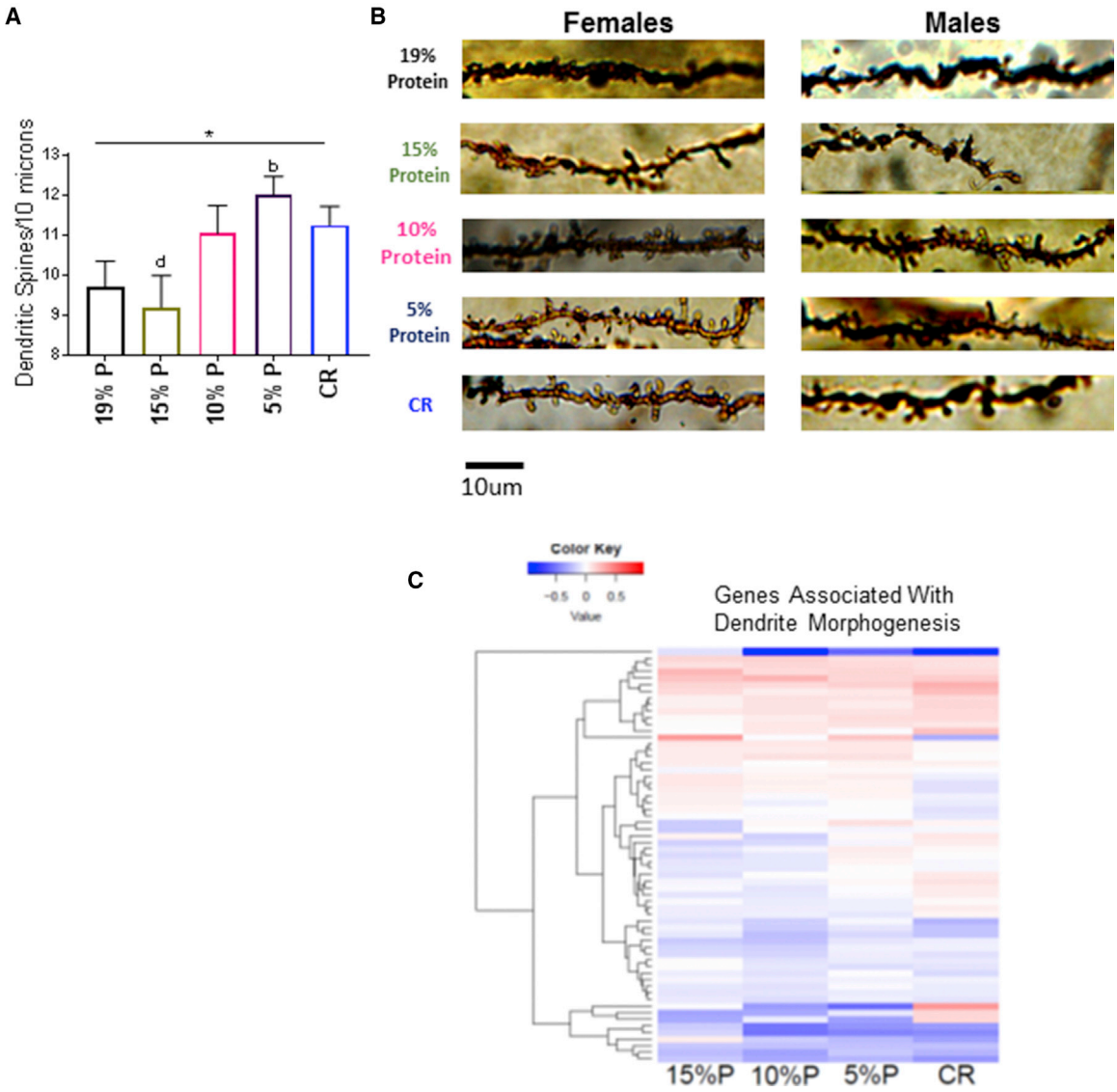

Figure 4. Dendritic Spine Density on Secondary and Tertiary Dendrites in the Hippocampal Dentate Gyrus and Related Genetic Expression at 15 Months of Age

(A) Dendritic spine density of DG neurons. n = 8–12 neurite segments per mouse from each group and 6 – 12 replicates per group depending on the stain quality.

(B) Representative images from dendritic spine segments from each experimental group, 15 months of age. Scale bar, 10 μm. See also Figure S2.

(C) Heatmap of upregulated or downregulated genes that are known to be dendrite morphogenesis. Each group is compared to control 19% protein diets, and the degree of relatedness among the genes is shown on the y axis. n = 6 replicates per group, 15 months of age, 14 months on diet. See also Table S10.

*p < 0.05; **p < 0.01; ***p < 0.001; ****p < 0.0001 ANOVA group analysis. a = significantly different to 19% P; b = significantly different to 15% P; c = significantly different to 10% P; d = significantly different to 5% P; e = significantly different to CR as determined by a Tukey's post hoc analysis. All data are represented by the mean ± SEM of the biological replicates.

one time point, 15 months, which represents late midlife, although our behavioral evaluation included 23-month-old mice. Future research should focus on older mice and models of neurodegenerative disease. We studied dendritic spine counts in the dentate gyrus because of its critical role in hippocampus-dependent brain function (Toda and Gage, 2017), but not other areas involved in memory formation (CA1 or CA3).

In conclusion, both CR and LPHC diets impacted on brain aging in the hippocampus. Although the behavioral and cognitive changes were subtle, there were more dramatic effects on gene expression, protein activity, and dendritic spine morphology. Overall, the lowest protein, highest carbohydrate diets (5% and 10% protein) generated changes, which approached those seen with CR. A very low-protein, high-carbohydrate diet may be a feasible nutritional intervention to delay brain aging.

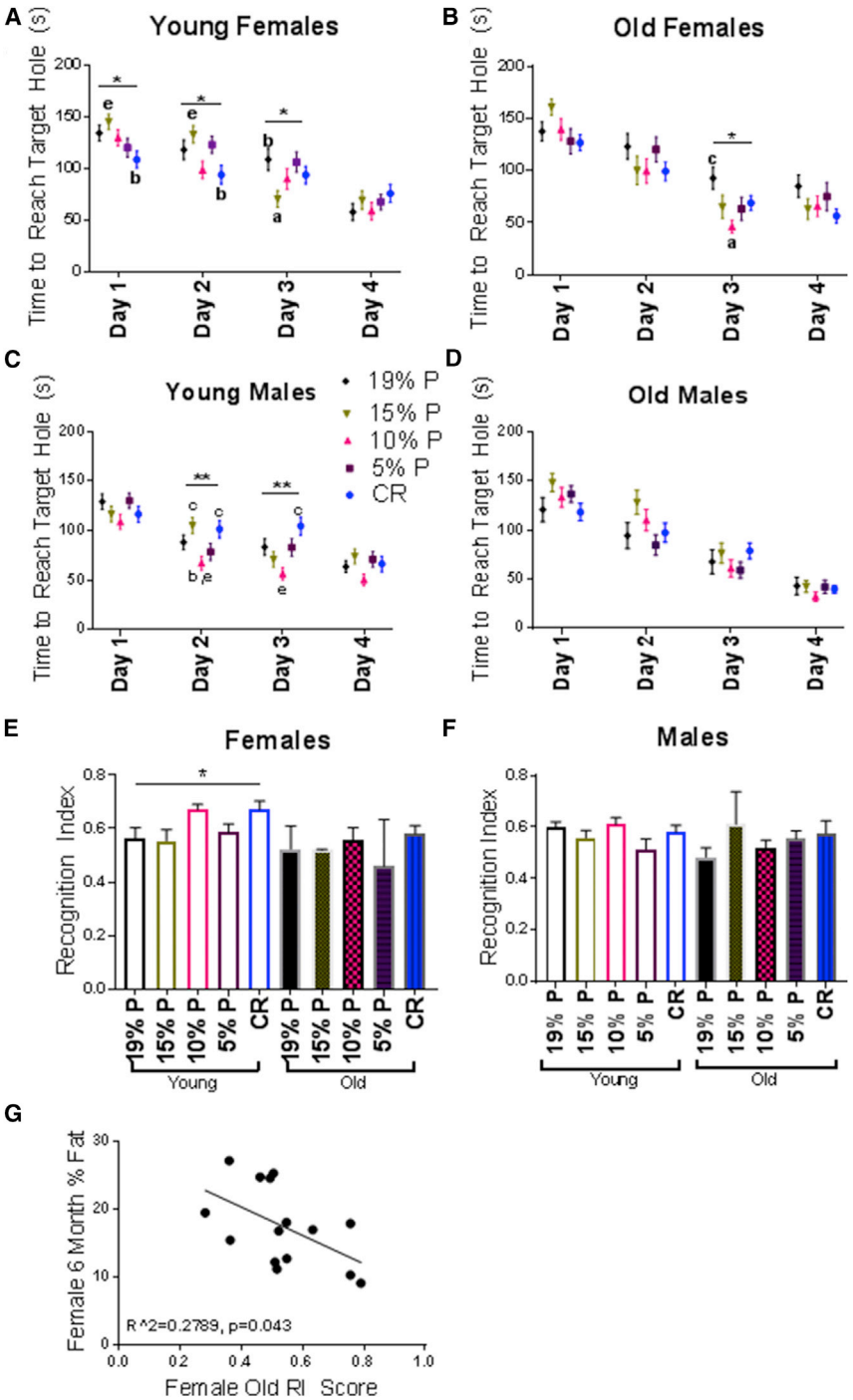

Figure 5. Behavioral and Cognitive Responses to CR and LPHC Diets at 13 and 23 Months of Age

(A) Barnes maze, 13-month-old females. Mean ± SEM of the time to reach the target hole. 4 trials per day, per mouse were completed. n = 12 mice per group.

(B) Barnes maze, 23-month-old females. n = 12 mice per group.

(C) Barnes maze, 13-month-old males. n = 12 mice per group.

(D) Barnes maze, 23-month-old males. n = 5–12 mice per group.

(E) Novel object recognition, 13- and 23-month-old females. Means ± SEM of the recognition index (RI), quantified by a ratio of new object exploration over total object exploration. n = 12 mice per group (young) and n = 5–12 mice per group (old).

(F) Novel object recognition, 13- and 23-month-old males. n = 12 mice per group (young) and n = 5–12 mice per group (old).

(G) Relationship between percent body fat at 6 months and RI score at 23 months, n = 15 females. *p < 0.05; **p < 0.01; ***p < 0.001; ****p < 0.0001 ANOVA group analysis. a = significantly different to 19% P; b = significantly different to 15% P; c = significantly different to 10% P; d = significantly different to 5% P; e = significantly different to CR as determined by a Tukey's post hoc analysis. All data are represented by the mean ± SEM.

STAR★METHODS

Detailed methods are provided in the online version of this paper and include the following:

- KEY RESOURCES TABLE
- CONTACT FOR REAGENT AND RESOURCE SHARING
- EXPERIMENTAL MODEL AND SUBJECT DETAILS
  - Animal husbandry and diets
- METHOD DETAILS
  - Animal sacrifice and tissue collection
  - Fat mass and lean mass
  - Metabolic measurements
  - Glucose tolerance

- Insulin determination
- FGF-21 assay
- Adiponectin determination
- Leptin determination
- Cholesterol, Albumin, ALT, Urea, and Triglycerides
- RNA isolation and processing
- RNA sequencing and analysis
- Protein isolation
- Western blots
- Milliplex map panel enzymatic activity assays
- BDNF enzymatic activity assay
- Golgi Staining
- Dendritic spine quantification
- Immunofluorescence
- Behavioral testing
- Novel Object Recognition (NOR)
- Barnes Maze (BM)

- QUANTIFICATION AND STATISTICAL ANALYSIS
- DATA SOFTWARE AND AVAILABILITY

SUPPLEMENTAL INFORMATION

Supplemental Information includes two figures and ten tables and can be found with this article online at https://doi.org/10.1016/j.celrep.2018.10.070.

ACKNOWLEDGMENTS

This work was supported by the National Health and Medical Research Council (project grant # 1084267) and funding from the Ageing and Alzheimers Association, the McKnight Bequest, the Sydney Medical School Foundation, and the American Australian Association. D.W. was partly funded by the American Australian Association. SMS-B is supported by an NHMRC Peter Doherty Biomedical Fellowship and a University of Sydney SOAR Fellowship. R.d.C. was funded by the Intramural Program of the National Institute on Aging, NIH. We thank Greg McIlwraith, Michael Kuligowski, Glen Lockwood, Nicholas Hunt, and Tim Dodgson. We thank Dr. Andrew Burgess and the ANZAC microscopy and flow facility for the assistance with the confocal microscopy and GFAP analysis. We thank the Laboratory Animal Services (LAS) at the University of Sydney and the Diagnostic Pathology Unit, Concord Hospital, and NSW Health.

AUTHOR CONTRIBUTIONS

S.M.S.-B., D.W., D.G.L., D.A.S., D.R., R.d.C., S.J.S., and V.C.C. conceived and designed the studies. S.M.S.-B., T.P., D.W., X.C., J.A.W., and G.J.C. performed most of the metabolic and systemic experiments. D.W. carried out all hippocampus and behavioral experiments and analyzed the associated data. Q.-P.W. carried out RNA-sequencing analysis. A.M.S. carried out additional statistical and mathematical data analysis. D.W., V.C.C., S.J.S., and D.G.L. wrote the manuscript. All authors contributed to reading, editing, and approving the final manuscript.

DECLARATION OF INTERESTS

The authors declare no competing interests.

Received: March 9, 2018
Revised: April 27, 2018
Accepted: October 19, 2018
Published: November 20, 2018

REFERENCES

Alavi, M.S., Shamsizadeh, A., Azhdari-Zarmehri, H., and Roohbakhsh, A. (2018). Orphan G protein-coupled receptors: the role in CNS disorders. Biomed. Pharmacother. *98*, 222–232.

Beste, C., Ocklenburg, S., von der Hagen, M., and Di Donato, N. (2016). Mammalian cadherins DCHS1-FAT4 affect functional cerebral architecture. Brain Struct. Funct. *221*, 2487–2491.

Bevins, R.A., and Besheer, J. (2006). Object recognition in rats and mice: a one-trial non-matching-to-sample learning task to study 'recognition memory'. Nat. Protoc. *1*, 1306–1311.

Brahmachari, S., Fung, Y.K., and Pahan, K. (2006). Induction of glial fibrillary acidic protein expression in astrocytes by nitric oxide. J. Neurosci. *26*, 4930–4939.

Buffa, R., Mereu, E., Putzu, P., Mereu, R.M., and Marini, E. (2014). Lower lean mass and higher percent fat mass in patients with Alzheimer's disease. Exp. Gerontol. *58*, 30–33.

Cheng, Y., Cawley, N.X., and Loh, Y.P. (2014). Carboxypeptidase E (NF-α1): a new trophic factor in neuroprotection. Neurosci. Bull. *30*, 692–696.

Dye, L., Boyle, N.B., Champ, C., and Lawton, C. (2017). The relationship between obesity and cognitive health and decline. Proc. Nutr. Soc. *76*, 443–454.

Eaton, S.L., Roche, S.L., Llavero Hurtado, M., Oldknow, K.J., Farquharson, C., Gillingwater, T.H., and Wishart, T.M. (2013). Total protein analysis as a reliable loading control for quantitative fluorescent Western blotting. PLoS ONE *8*, e72457.

Garcia, J.M., Stillings, S.A., Leclerc, J.L., Phillips, H., Edwards, N.J., Robicsek, S.A., Hoh, B.L., Blackburn, S., and Doré, S. (2017). Role of interleukin-10 in acute brain injuries. Front. Neurol. *8*, 244.

Gewurz, B.E., Towfic, F., Mar, J.C., Shinners, N.P., Takasaki, K., Zhao, B., Cahir-McFarland, E.D., Quackenbush, J., Xavier, R.J., and Kieff, E. (2012). Genome-wide siRNA screen for mediators of NF-κB activation. Proc. Natl. Acad. Sci. USA *109*, 2467–2472.

Hadem, I.K.H., Majaw, T., Kharbuli, B., and Sharma, R. (2017). Beneficial effects of dietary restriction in aging brain. J. Chem. Neuroanat. Published online October 12, 2017. https://doi.org/10.1016/j.jchemneu.2017.10.001.

Ingram, D.K., Weindruch, R., Spangler, E.L., Freeman, J.R., and Walford, R.L. (1987). Dietary restriction benefits learning and motor performance of aged mice. J. Gerontol. *42*, 78–81.

Jacobs, B., Johnson, N.L., Wahl, D., Schall, M., Maseko, B.C., Lewandowski, A., Raghanti, M.A., Wicinski, B., Butti, C., Hopkins, W.D., et al. (2014). Comparative neuronal morphology of the cerebellar cortex in afrotherians, carnivores, cetartiodactyls, and primates. Front. Neuroanat. *8*, 24.

Kesner, R.P. (2018). An analysis of dentate gyrus function (an update). Behav. Brain Res. *354*, 84–91, Published online July 26, 2017. https://doi.org/10.1016/j.bbr.2017.07.033.

Kim, Y.N., Jung, H.Y., Eum, W.S., Kim, D.W., Shin, M.J., Ahn, E.H., Kim, S.J., Lee, C.H., Yong, J.I., Ryu, E.J., et al. (2014). Neuroprotective effects of PEP-1-carbonyl reductase 1 against oxidative-stress-induced ischemic neuronal cell damage. Free Radic. Biol. Med. *69*, 181–196.

Le Couteur, D.G., Solon-Biet, S., Cogger, V.C., Mitchell, S.J., Senior, A., de Cabo, R., Raubenheimer, D., and Simpson, S.J. (2016). The impact of low-protein high-carbohydrate diets on aging and lifespan. Cell. Mol. Life Sci. *73*, 1237–1252.

Mattson, M.P. (2010). The impact of dietary energy intake on cognitive aging. Front. Aging Neurosci. *2*, 5.

Mattson, M.P., Moehl, K., Ghena, N., Schmaedick, M., and Cheng, A. (2018). Intermittent metabolic switching, neuroplasticity and brain health. Nat. Rev. Neurosci. *19*, 63–80.

Mazucanti, C.H., Cabral-Costa, J.V., Vasconcelos, A.R., Andreotti, D.Z., Scavone, C., and Kawamoto, E.M. (2015). Longevity pathways (mTOR, SIRT, Insulin/IGF-1) as key modulatory targets on aging and neurodegeneration. Curr. Top. Med. Chem. *15*, 2116–2138.

Mitchell, S.J., Madrigal-Matute, J., Scheibye-Knudsen, M., Fang, E., Aon, M., González-Reyes, J.A., Cortassa, S., Kaushik, S., Gonzalez-Freire, M., Patel, B., et al. (2016). Effects of sex, strain, and energy intake on hallmarks of aging in mice. Cell Metab. *23*, 1093–1112.

Newman, J.C., Covarrubias, A.J., Zhao, M., Yu, X., Gut, P., Ng, C.P., Huang, Y., Haldar, S., and Verdin, E. (2017). Ketogenic diet reduces midlife mortality and improves memory in aging mice. Cell Metab. *26*, 547–557.e8.

Nikonova, E.V., Gilliland, J.D., Tanis, K.Q., Podtelezhnikov, A.A., Rigby, A.M., Galante, R.J., Finney, E.M., Stone, D.J., Renger, J.J., Pack, A.I., et al. (2017). Transcriptional profiling of cholinergic neurons from basal forebrain identifies changes in expression of genes between sleep and wake. Sleep *40*. https://doi.org/10.1093/sleep/zsx059.

Orlowski, D., and Bjarkam, C.R. (2012). A simple reproducible and time saving method of semi-automatic dendrite spine density estimation compared to manual spine counting. J. Neurosci. Methods *208*, 128–133.

Pani, G. (2015). Neuroprotective effects of dietary restriction: evidence and mechanisms. Semin. Cell Dev. Biol. *40*, 106–114.

Paradis, S., Harrar, D.B., Lin, Y., Koon, A.C., Hauser, J.L., Griffith, E.C., Zhu, L., Brass, L.F., Chen, C., and Greenberg, M.E. (2007). An RNAi-based approach identifies molecules required for glutamatergic and GABAergic synapse development. Neuron *53*, 217–232.

Parrella, E., Maxim, T., Maialetti, F., Zhang, L., Wan, J., Wei, M., Cohen, P., Fontana, L., and Longo, V.D. (2013). Protein restriction cycles reduce IGF-1 and phosphorylated Tau, and improve behavioral performance in an Alzheimer's disease mouse model. Aging Cell *12*, 257–268.

Plank, M., Wuttke, D., van Dam, S., Clarke, S.A., and de Magalhães, J.P. (2012). A meta-analysis of caloric restriction gene expression profiles to infer common signatures and regulatory mechanisms. Mol. Biosyst. *8*, 1339–1349.

Prolla, T.A., and Mattson, M.P. (2001). Molecular mechanisms of brain aging and neurodegenerative disorders: lessons from dietary restriction. Trends Neurosci. *24* (*11, Suppl*), S21–S31.

Ren, H., Orozco, I.J., Su, Y., Suyama, S., Gutiérrez-Juárez, R., Horvath, T.L., Wardlaw, S.L., Plum, L., Arancio, O., and Accili, D. (2012). FoxO1 target Gpr17 activates AgRP neurons to regulate food intake. Cell *149*, 1314–1326.

Schafer, M.J., Dolgalev, I., Alldred, M.J., Heguy, A., and Ginsberg, S.D. (2015). Calorie restriction suppresses age-dependent hippocampal transcriptional signatures. PLoS ONE *10*, e0133923.

Simpson, J., and Kelly, J.P. (2012). An investigation of whether there are sex differences in certain behavioural and neurochemical parameters in the rat. Behav. Brain Res. *229*, 289–300.

Simpson, S.J., Le Couteur, D.G., Raubenheimer, D., Solon-Biet, S.M., Cooney, G.J., Cogger, V.C., and Fontana, L. (2017). Dietary protein, aging and nutritional geometry. Ageing Res. Rev. *39*, 78–86.

Simpson, S.J., and Raubenheimer, D. (2012). The Nature of Nutrition: A Unifying Framework from Animal Nutrition to Human Obesity (Princeton University Press).

Solon-Biet, S.M., McMahon, A.C., Ballard, J.W., Ruohonen, K., Wu, L.E., Cogger, V.C., Warren, A., Huang, X., Pichaud, N., Melvin, R.G., et al. (2014). The ratio of macronutrients, not caloric intake, dictates cardiometabolic health, aging, and longevity in ad libitum-fed mice. Cell Metab. *19*, 418–430.

Solon-Biet, S.M., Mitchell, S.J., Coogan, S.C., Cogger, V.C., Gokarn, R., McMahon, A.C., Raubenheimer, D., de Cabo, R., Simpson, S.J., and Le Couteur, D.G. (2015). Dietary protein to carbohydrate ratio and caloric restriction: comparing metabolic outcomes in mice. Cell Rep. *11*, 1529–1534.

Solon-Biet, S.M., Cogger, V.C., Pulpitel, T., Heblinski, M., Wahl, D., McMahon, A.C., Warren, A., Durrant-Whyte, J., Walters, K.A., Krycer, J.R., et al. (2016). Defining the nutritional and metabolic context of FGF21 using the Geometric Framework. Cell Metab. *24*, 555–565.

Sørensen, A., Mayntz, D., Raubenheimer, D., and Simpson, S.J. (2008). Protein-leverage in mice: the geometry of macronutrient balancing and consequences for fat deposition. Obesity (Silver Spring) *16*, 566–571.

Stranahan, A.M., Lee, K., Martin, B., Maudsley, S., Golden, E., Cutler, R.G., and Mattson, M.P. (2009). Voluntary exercise and caloric restriction enhance hippocampal dendritic spine density and BDNF levels in diabetic mice. Hippocampus *19*, 951–961.

Sunyer, B., Patil, S., Höger, H., and Lubec, G. (2007). Barnes maze, a useful task to assess spatial reference memory in the mice. Nature, Published online October 4, 2007. https://doi.org/10.1038/nprot.2007.390.

Testa, G., Biasi, F., Poli, G., and Chiarpotto, E. (2014). Calorie restriction and dietary restriction mimetics: a strategy for improving healthy aging and longevity. Curr. Pharm. Des. *20*, 2950–2977.

Tian, Q., An, Y., Resnick, S.M., and Studenski, S. (2017). The relative temporal sequence of decline in mobility and cognition among initially unimpaired older adults: results from the Baltimore Longitudinal Study of Aging. Age Ageing *46*, 445–451.

Toda, T., and Gage, F.H. (2017). Review: adult neurogenesis contributes to hippocampal plasticity. Cell Tissue Res. *373*, 693–709.

Tolppanen, A.M., Ngandu, T., Kåreholt, I., Laatikainen, T., Rusanen, M., Soininen, H., and Kivipelto, M. (2014). Midlife and late-life body mass index and late-life dementia: results from a prospective population-based cohort. J. Alzheimers Dis. *38*, 201–209.

Valencak, T.G., Osterrieder, A., and Schulz, T.J. (2017). Sex matters: The effects of biological sex on adipose tissue biology and energy metabolism. Redox Biol. *12*, 806–813.

Wahl, D., Cogger, V.C., Solon-Biet, S.M., Waern, R.V., Gokarn, R., Pulpitel, T., Cabo, Rd., Mattson, M.P., Raubenheimer, D., Simpson, S.J., and Le Couteur, D.G. (2016). Nutritional strategies to optimise cognitive function in the aging brain. Ageing Res. Rev. *31*, 80–92.

Wahl, D., Coogan, S.C., Solon-Biet, S.M., de Cabo, R., Haran, J.B., Raubenheimer, D., Cogger, V.C., Mattson, M.P., Simpson, S.J., and Le Couteur, D.G. (2017). Cognitive and behavioral evaluation of nutritional interventions in rodent models of brain aging and dementia. Clin. Interv. Aging *12*, 1419–1428.

Walker, D.G., Whetzel, A.M., and Lue, L.F. (2015). Expression of suppressor of cytokine signaling genes in human elderly and Alzheimer's disease brains and human microglia. Neuroscience *302*, 121–137.

Willette, A.A., Coe, C.L., Birdsill, A.C., Bendlin, B.B., Colman, R.J., Alexander, A.L., Allison, D.B., Weindruch, R.H., and Johnson, S.C. (2013). Interleukin-8 and interleukin-10, brain volume and microstructure, and the influence of calorie restriction in old rhesus macaques. Age (Dordr.) *35*, 2215–2227.

Wood, S.H., van Dam, S., Craig, T., Tacutu, R., O'Toole, A., Merry, B.J., and de Magalhães, J.P. (2015). Transcriptome analysis in calorie-restricted rats implicates epigenetic and post-translational mechanisms in neuroprotection and aging. Genome Biol. *16*, 285.

Zaqout, S., and Kaindl, A.M. (2016). Golgi-Cox staining step by step. Front. Neuroanat. *10*, 38.

Zeier, Z., Madorsky, I., Xu, Y., Ogle, W.O., Notterpek, L., and Foster, T.C. (2011). Gene expression in the hippocampus: regionally specific effects of aging and caloric restriction. Mech. Ageing Dev. *132*, 8–19.

Zhang, B., Bailey, W.M., Braun, K.J., and Gensel, J.C. (2015). Age decreases macrophage IL-10 expression: Implications for functional recovery and tissue repair in spinal cord injury. Exp. Neurol. *273*, 83–91.

STAR★METHODS

KEY RESOURCES TABLE

REAGENT or RESOURCE	SOURCE	IDENTIFIER
Antibodies		
Phospho-mTOR (Ser2448) Antibody	Cell Signaling Technology	#2971; RRID:AB_330970
mTOR (7C10) Rabbit mAb	Cell Signaling Technology	#2983; RRID:AB_2105622
SirT1 (D1D7) Rabbit mAb	Cell Signaling Technology	#9475; RRID:AB_2617130
β-Actin (13E5) Rabbit mAb	Cell Signaling Technology	#4970; RRID:AB_2223172
Anti-Drebrin antibody	abcam	ab60933; RRID:AB_10675963
Anti-GAPDH antibody - Loading Control	abcam	ab9485; RRID:AB_307275
Anti-PGC1 alpha antibody	abcam	ab54481; RRID:AB_881987
Anti-rabbit IgG, HRP-linked Antibody	Cell Signaling Technology	#7074; RRID:AB_2099233
Rabbit Polyclonal Anti-Iba1 antibody	GeneTex	GTX100042; RRID:AB_1240434
Rabbit Polyclonal Anti-GFAP antibody	Abcam	ab7260; RRID:AB_305808
Goat anit-Rabbit IgG (H+L) Cross-Adsorbed Secondary Antibody, Cyanine3	ThermoFisher Scientific	A10520; RRID:AB_2534029
VECTASHIELD Antifade Mounting Medium with DAPI	Vector Laboratories	H-1200; RRID:AB_2336790
Chemicals, Peptides, and Recombinant Proteins		
DPX Mounting Media for histology	Sigma-Aldrich	06522
cOmplete, EDTA-free Protease Inhibitor Cocktail	Sigma-Aldrich	COEDTAF-RO ROCHE
10x Tris Buffered Saline (TBS)	Bio-Rad	#1706435
TRI Reagent® for DNA, RNA and protein isolation	Sigma-Aldrich	93289
Ponceau S Dye	Sigma-Aldrich	P7170
Critical Commercial Assays		
FD Rapid GolgiStain Kit (large)	FD Neurotechnologies	PK401
BDNF E_{max}® ImmunoAssay Systems	Promega	G7610
MCYTOMAG-70K | MILLIPLEX MAP Mouse Cytokine/Chemokine Magnetic Bead Panel - Immunology Multiplex Assay	Merck Millipore	# MCYTOMAG
Pierce BCA Protein Assay Kit	Thermo Fisher Scientific	23225
Mouse Leptin ELISA Kit	Crystal Chem High Performance Assays	90030
Mouse Adiponectin ELISA Kit	Crystal Chem High Performance Assays	80569
Fibroblast Growth Factor 21 Mouse/Rat ELISA	BioVendor Research and Diagnostic Products	RD291108200R
Ultra Sensitive Mouse Insulin ELISA Kit	Crystal Chem High Performance Assays	90080
Deposited Data		
Raw sequence data deposited into NCBI	Total Hippocampus RNA	GEO: GSE111778
Experimental Models: Organisms/Strains		
C57/b6 male and female mice	Animal Resource Centre, Perth, WA	N/A
Software and Algorithms		
NeuronStudio	Mount Sanai School of Medicine, freely available available online	http://research.mssm.edu/cnic/tools-ns.html
ImageJ	National Institutes of Health, freely available online	https://imagej.nih.gov/ij/
AnyMaze behavioral tracking software	Stoelting Co. Wood Dale, IL.	http://www.anymaze.co.uk/
The R Project for statistical computing	Freely available online	https://www.r-project.org/
GraphPad Prism Software	Available for download online	https://www.graphpad.com/scientific-software/prism/

CONTACT FOR REAGENT AND RESOURCE SHARING

Further information and requests for resources and reagents should be directed to and will be fulfilled by the Lead Contact, Professor David G. Le Couteur (david.lecouteur@sydney.edu.au).

EXPERIMENTAL MODEL AND SUBJECT DETAILS

Animal husbandry and diets

Animals were purchased from the Animal Resource Centre (Perth, WA) and housed four per cage on a 12-hour light/dark cycle at 22-24°C at the Charles Perkins Centre at The University of Sydney. All animals were given free access to water and randomly assigned to experimental groups. *Ad-libitum* animals were given free-access to food while CR animals were given an allotment with 20% fewer calories than the average intake of their *ad-libitum* 19% protein counterparts daily at 3.00pm. Mice were weaned at 3 weeks of age and diets were started at approximately three months of age. Energy intake from each macronutrient was determined and averaged daily from 12 – 15 months of age. Body weights were taken every two weeks and animals were routinely monitored every week for general health. The ethics in this study were approved by the University of Sydney, animal ethics number 2014/752.

Diets were purchased from Specialty Feeds (Perth, Western Australia) and formulated to have the same total energy content (isocaloric) but different ratios in protein to carbohydrate with fixed fat (Table 1). Each diet was based on the rodent diet AIN-93G (Specialty Feeds) and formulated to contain all essential vitamins, minerals, and amino acids for growth in mice. The primary dietary protein component was casein, the main carbohydrate component was starch, and the main fat component was soy oil.

METHOD DETAILS

Animal sacrifice and tissue collection

At 15 months of age a subset (n = 12 males, n = 12 females per group) of mice were culled. All animals were sacrificed between the hours of 10am and 12 noon. Animals were sacrificed in randomized order to minimize experimental bias. After deep anesthetizing with xylazine-ketamine (10mg/g bw), approximately 1 mL of blood was taken via cardiac puncture. The liver was removed, weighed, and flash-frozen in liquid nitrogen. The mice were then decapitated and the brain was carefully removed. One-half of the brain was immediately washed with ice-cold double-deionized water and placed into Golgi-Cox solution. The whole hippocampus was carefully dissected from the other half, immediately snap-frozen in liquid-nitrogen, and moved to −80°C until further processing. The blood was placed into a ice-cold tube and placed directly into wet ice before centrifugation at 14,000 rpm for 10 minutes for plasma collection. The plasma was used for subsequent metabolic and systemic measurements. Males and females were analyzed separately on metabolic measurements due to innate metabolic differences between sexes (Valencak et al., 2017).

Fat mass and lean mass

Fat mass and lean mass were measured by magnetic resonance imaging (EchoMRI 900 – EchoMRI LLC, Houston, Texas, USA). The mice were awake during the process and snuggly put into a plastic tube before being placed inside the machine for approximately 1 minute. The machine calculated the fat mass (g) and lean mass (g) per each mouse.

Metabolic measurements

The respiratory quotient was measured by Metabolic Cage (Promethion, Sable Systems International, Las Vegas, NV, USA). Briefly, individual mice were placed in each cage and acclimatized for 8 hours then left for 48 hours (2 dark and 2 light cycles). Calorimetric data were calculated with the software and the average respiratory quotient was obtained during the dark cycle. Data are presented as CO_2 eliminated/O_2 consumed (Respiratory quotient; RQ).

Glucose tolerance

Glucose tolerance was measured at 15 months of age. Mice were fasted for 6 hours before the test which took place in the afternoon at 2.00 pm. Mice were orally gavaged with glucose (2 g/kg lean mass) and blood glucose levels were read by tail snip at time 0, 15 min, 30 min, 45 minutes, 60 minutes, and 90 minutes (Accu-Check Performa, Roche, Australia). The total area under the curve (AUC) was calculated and data are presented as mm/l.min.

Insulin determination

Total fasting insulin levels were measured with an ultra-sensitive mouse insulin ELISA kit per manufacturer's instructions (Chrystal Chem, Elk Grove Village, IL, USA). Whole blood was added to each well in the 96-well plate containing 90 μL of the provided diluent "G." 10 μL of blood was collected by tail snip and added to each well. The "mouse insulin standard" was reconstituted and the standards were mixed (from 0.1 ng/mL to 6.4 ng/mL). 95 μL of the provided diluent and 5 μl of each standard was added into each well, the plate was covered, and incubated overnight at 4°C. The plate was removed from 4°C and washed 5 times with 250 μl wash buffer and 100 μl of the anti-inulin conjugate was added to each well. The plate was covered and incubated for 30 minutes at room temperature and subsequently washed 7 times with 250 μL wash buffer in each well. 100 μl of the enzyme substrate was

added to each well, covered in the dark for 40 minutes, and the reaction ended with the addition of 100 μl stop solution "F." The plate was read at an absorbance of A450-A630 and insulin concentration was determined by linear fit. Data are presented as ng/mL.

FGF-21 assay

The Fibroblast Growth Factor-21 assay was analyzed by ELISA (Biovendor, Karasek, Czech Republic). The mouse master standards were reconstituted with the provided dilution buffer (40 pg/mL – 2568 pg/mL). 100 μl of standards and diluted samples (serum diluted in dilution buffer) were added to each appropriate well. The plate was incubated at room temperature for one hour with shaking at 300 rpm and washed three times with the provided wash buffer. 100 ul of biotin-labeled antibody was subsequently added to each well and incubated for one hour at room temperature with shaking. The wells were washed 3x with the wash buffer and 100 μL of Sterptavidin-HRP conjugate was added to each well and incubated with shaking for 30 minutes. The plate was washed 3x with wash buffer and 100 μl of substrate solution was added to each well, covered in foil, and incubated at room temperature for 10 minutes, and the reaction was stopped by the addition of 100 μl of stop solution. The absorbance of each well was determined by reading on a microplate reader at 550 – 650 nm and concentrations were determined with the standard curve. Data are presented serum FGF-21 concentration in pg/mL.

Adiponectin determination

Adiponectin concentrations were determined using a mouse adiponectin ELISA kit (Crystal Chem, Elk Grove Village, Il, USA). The mouse standards were reconstructed from the provided stock (0.025 – 1 ng/mL). Serum samples were diluted to the appropriate concentration (1:10,000) in the dilution buffer. 100 μL of sample and each standard were added to each well and incubated for 1 hour at RT with shaking for 350 RPM. The plate was washed 3x and 100ul of the provided antibody conjugate was added to each well and incubated for 1 hour with shaking at 350 rpm. The plate was washed 3x with wash buffer, 100 μL of substrate solution was added and incubated for 30 minutes. 100 μL of stop solution was added and the OD was measured at 460/630 nm. Data are presented as the Adiponectin concentration in ng/mL.

Leptin determination

Leptin concentrations were determined using a mouse leptin ELISA kit (Crystal Chem, Elk Grove Village, Il, USA). The mouse standards were reconstructed from the provided stock (0.0 – 12.8 ng/mL) and serum samples were diluted to the appropriate concentrations. 100 μL of each standard or sample was added to each well and incubated overnight at 4°C. The plate was then washed and 100 μL of the conjugate solution was added followed by 4 hours of incubation at 4°C. The plate was washed and 100 μL of the substrate solution was added, incubated for 30 minutes, and 100 μL of stop solution was added to each well. The plate was read on a spectrometer at an OD of 450/630 nm. Data are presented as serum leptin levels in ng/mL.

Cholesterol, Albumin, ALT, Urea, and Triglycerides

Serum cholesterol, albumin, ALT, urea, and triglyceride levels were analyzed by a Cobas 8000, c702 photometric module (Hitachi, Japan) and all reagents were provided by Roche (Roche diagnostics, Germany). All analyses were completed at Concord Hospital (NSW, Australia).

RNA isolation and processing

RNA was isolated using the *Trizol* method. 1mL of ice-cold TRIzol reagent (Sigma Aldrich, St. Louis, MO, USA) was added to fresh-frozen whole hippocampus. Tissue was homogenized using the bead method (QIAGEN, Hilden, Germany) for 30 s at 50 *Hz*. After samples were let to sit on ice for 10 minutes, 200 μl of ice-cold chloroform was added and samples were let to sit at room temperature for an additional 3 minutes. Samples were centrifuged at 14,000 rpm for 20 minutes and approximately 500 μL of the supernatant was collected and added to an equal volume of ice-cold 2-propanol. Samples were mixed, placed directly on ice, and centrifuged at 14,000 RPM for 20 minutes. The supernatant was removed and the remaining pellet was washed with 500 μL of ice-cold ethanol 3 times before air-drying. The pellet was resuspended in 15 μL nuclease-free water and cleaned with DNase (Invitrogen, Carlsbad, CA, USA). RNA purity was assessed using a nanodrop spectrometer (Thermofisher Scientific Australia) before freezing at −80°C until further analysis.

RNA sequencing and analysis

Samples were processed by The Australian Genome Research Facility (AGRF - Victoria, Australia; http://www.agrf.org.au/) with Illumina TruSeq stranded mRNA sample preparation and technology. RNA integrity was initially assessed by a bioanalyzer and all samples passed quality control with RIN values $\geq$ 8.0 and an A260/280 ratio of 1.8 – 2.0. Briefly, mRNA was purified via oligo(dT) beads followed by fragmentation of mRNA with divalent cations and heat. 1st strand cDNA synthesis was randomly primed followed by second strand cDNA synthesis. cDNA library preparation was prepared first by DNA fragment end repair followed by 3′ adenylation of DNA fragments and subsequent sequencing adaptor ligation. Finally, the library was amplified by PCR.

Primary sequence data were generated using the Illumina bcl2fastq 2.19.0.12 pipeline and sequence reads from all samples were analyzed per AGRF quality control measures. Briefly, cleaned sequence reads were aligned against the *Mus musculus* genome (Build version mm10). The Tophat aligner (v2.0.14) was used to map reads to the genomic sequences. The raw gene reads were generated

by featureCounts (v1.4.6) and the differential gene expression was analyzed by DESeq2 (v1.16.1) in R (package v3.4.0). The Gene Set Enrichment analysis (GSEA) was completed by a SetRank method (PMID: 28259142). The heatmaps and Venn Diagrams were generated in R (package v3.4.0). The heatmaps were generated from FPKM values of the genes that were considered significant compared to the 19% protein group. For each heatmap, the red, white, and blue colors indicate higher than mean, close to mean, and lower than mean expression of a particular gene, respectively, as measured by the row of standardized Z-scores. The rows are organized by hierarchical clustering using agglomerative clustering with complete linkage and Euclidian distance metric. The volcano plot and Venn diagrams were constructed by a Pearson calculation with the top 2.5% of genes in either direction considered significant. All genetic data are available at the online database GEO: GSE111778.

Protein isolation

Whole frozen hippocampus was homogenized using the bead method for 50hz for 30 s (QIAGEN TissueLyser LT) in 500 μL ice-cold RIPA buffer containing Tris-HCl, NaCl, Triton X-100, Na-deoxycholate, SDS, and fresh protease and phosphatase inhibitor tablets (Roche cOmplete, EDTA-free Protease Inhibitor Cocktail). The tissue was let to sit on ice for 10 minutes followed by 20 minutes of centrifugation at 14,000 rpm. The supernatant was transferred to a fresh ice-cold tube and protein concentrations were assessed using a bicinchoninic acid (BCA) assay (Thermo Scientific, Pierce BCA Protein Assay Kit). Samples were then diluted to approximately the same concentrations before being stored at minus 80°C until further analysis. Protein lysates were used for subsequent enzymatic activity assays, Milliplex Map Panels, and western blots.

Western blots

Lysates were prepared for bis/tris polyacrylamide gel electrophoresis under reduced conditions. Proteins were transferred to nitrocellulose membranes (Invitrogen) and immediately stained with Ponceau S dye (Sigma Aldrich, St. Louis, MO, USA) for rapid and reversible visualization of total protein per lane. Protein expression was detected using specific primary antibodies. Antibodies raised against p-MTOR (#2971; 1:000), MTOR (#2983; 1:1000), SIRT1 (#9475; 1:750), and β-ACTIN (#4970; 1:1000) were purchased from Cell Signaling Technology (Danvers, MA, USA). Antibodies raised against DREBRIN (ab60933; 1:000), GAPDH (ab9485; 1:1000), and PGC1-α (ab54481; 1:1000) were purchased from abcam (Cambridge, UK). All antibodies were detected using secondary rabbit IgG-horse radish peroxidase (#7074; 1:5000) purchased from Cell-Signaling and visualized by enhanced chemiluminescence (GE Healthcare, Chicago, IL, USA). Levels of specific proteins were normalized to total protein as visualized to ponceau S staining (Eaton et al., 2013) and band densitometric values analyzed with ImageJ (National Institutes of Health, Bethesda, MD). Loading controls GAPDH and ACTIN bands are shown along with their representative blots solely for comparison purposes.

Milliplex map panel enzymatic activity assays

Levels of IL-6, IL-10, and TNFα were assessed using the mouse cytokine/chemokine magnetic bead panel 96-Well Plate Assay (Cat # MCYTOMAG – 70K, EMD Millipore Corporation, Billerica, MA, USA) per manufacturer's instructions. After a plate wash, 25ul of each standard or control was added to the appropriate wells followed by 25 μL of assay buffer to the sample wells. 25 μL of whole hippocampal tissue lysates were added to the appropriate wells followed by 25 μL of premixed cytokine panel beads. The plate was sealed, covered with aluminum foil, and incubated overnight at 4°C. The following day the plate was removed from 4°C and washed 2 times with the provided wash buffer. 25 μL of detection antibodies were added to each well and the plate was covered with foil and incubated with shaking for 1 hour at RT. 25 μL of Streptavidin-Phycoerythrin was then added to each well, covered with foil, and incubated with shaking for 30 minutes. The plate was then washed 2 times and 150 μL of the provided drive fluid was added to each well followed by 5 minutes of shaking. The plate was run and read on MAGPIX® machine with xPonenent® Software (EMD Millipore Corporation, Billerica, MA, USA). The data were analyzed using Xponent® software. Briefly, the software analyzed median fluorescent intensity data using 5-parameter logistic or spline curve-fitting method for calculating each cytokine concentration in samples. Data are presented as ng/mg protein.

BDNF enzymatic activity assay

The BDNF ImmunoAssay Elisa was performed per manufacturer's instructions (Promega Corporation, Madison, WI, USA). Flat-bottom 96-well plates were coated with Anti-BDNF Monoclonal Antibody overnight at 4°C to bind soluble antibody. After the addition of 25 μL of each standard or lysate, the plate was incubated for 2 hours and secondary antibody was added. The plate was washed 3 times with TBS-T and the amount of bound pAb was detected using an anti-IgY horseradish peroxidase antibody. Unbound conjugate was removed by washing 5 times with TBST, a chomogenic substrate was added, and color was measured on a spectrometer at a wavelength of 450nm. Data are presented as mg BDNF/μg protein.

Golgi Staining

A rapid Golgi Stain was performed per manufacturer's instructions (FD Neurotechnologies, Inc, Columbia, MD, USA). Brains were removed and rinsed with ice-cold double deionized water. The complete right section was submerged in an impregnation solution consisting of equal parts of solution 'A' and solution 'B'. Samples were stored at room temperature in the dark for 2 weeks and then moved to solution 'C' for 3 days. They were then cut on the midsagittal plane with a vibratome at 100 μm to visualize and quantify dendritic spines (Zaqout and Kaindl, 2016). Samples were left to dry before the staining protocol. Sections were rinsed in distilled

water before placing into a mixture consisting of 1 part solution 'D' and 1 part solution 'E'. After an additional rinse, sections were dehydrated in increasing 50%, 75%, and 95% ethanol solutions before clearing in xylene and coverslipping in DPX mounting media for histology (Sigma Aldrich, St. Louis, MO, USA).

Dendritic spine quantification

Slides were imaged on an Olympus VS-120 Slide Scanner at 40X magnification which gave good resolution for spine counting purposes (Orlowski and Bjarkam, 2012). 25 z-slices of 1 μm each were imaged from each hippocampus. Dendritic spines were quantified using NeuronStudio software (Mount Sanai School of Medicine, available at http://research.mssm.edu/cnic/tools-ns.html) and blindly counted (DW). It has been demonstrated that the manual counting method by an investigator does not produce significantly different results when compared to other software or semi-automatic counting methods (Orlowski and Bjarkam, 2012). Spines were quantified in the dentate gyrus of each hippocampus and secondary and tertiary branches of each neuron were analyzed. A total of 8 - 12 segments were quantified from each hippocampus depending on the quality of the stain. The quantified dendritic branch segments were required to have the characteristics as previously described (Jacobs et al., 2014): (1) completely and darkly stained near the center of the 100 μm section, (2) contain no broken sections with complete spines, and (3) isolated without interference or overlap from other structures. Data are presented at the number of spines per 10 microns (Stranahan et al., 2009).

Immunofluorescence

Brains were carefully removed and cut on a midsagittal plane. The left side was placed in 4% formalin for 24 hours followed by 30% sucrose cryoprotection for 24 hours at 4°C. Brains were embedded in OCT (Siltera-Finetele, Inc, USA, Torrance, CA) before slowly freezing on dry ice and storing at −80°C until further use. They were sliced at 30 μm on a midsagittal plane on a cryostat. 5 sections were taken from each brain and mounted on slides. For Iba1 staining, sections were post-fixed with 4% PFA before quenching with 50 mM NH_4CL. For antigen retrieval, a commercially available Proteinase K solution was used for three minutes (Sigma Aldrich, St. Louis, MO, USA) and tissue was blocked for 30 minutes with 10% goat serum in PBS. Slides were incubated with primary antibodies Iba1 (1:250; GeneTex Irvine, CA, USA) overnight at 4°C. Sections were thoroughly washed and incubated with the fluorescent secondary antibody (1:1000, Cyanine 3, ThermoFisher Scientific) for 1 hour before washing and coverslipping with vectashield mounting media containing DAPI (Vector Laboratories, Burlingame, CA, USA). For GFAP, slides were washed with PBST before blocking for 30 minutes in 3% goat serum in PBS. Slides were placed into primary antibody (1:2000, abcam, United States) diluted in 3% goat serum in PBS. Slides were incubated overnight at 4 degrees followed by washing with PBST and a 1 hour incubation in secondary antibody (1:1000; Cyanine3, ThermoFisher Scientific) for one hour. Slides were imaged on a on an Olympus VS-120 Slide Scanner at 20X magnification (Iba1) or a Leica confocal microscope with white light laser (WLL), coupled with a 20X HC PL APO CS2 NA 0.75 lens (GFAP). Images were quantified using ImageJ. Data are presented as the number of $Iba1^+$ cells per $1mm^2$ in the hippocampus or the mean corrected total hippocampus fluorescence (GFAP).

Behavioral testing

Animals were handled extensively before and during the testing phase to acclimatize them to human interaction and minimize potential anxiety caused by interference. Mice received a minimum 2-hours of room habituation before commencing each test. Animals were tested in random order during each testing period and equipment was thoroughly cleaned with 80% ethanol between trials to minimize scents. To test memory during aging animal performance was assessed on both the Novel Object Recognition and Barnes Maze memory tasks. The same animals were tested at young and old age in a longitudinal manner, similar to human dementia and memory studies (Tian et al., 2017). The two-time points were 13 months of age (young) and 23 months of age (old). Animals received a minimum 3 days rest in between the two tests. Male and female results were analyzed separately because of innate behavioral and response differences between sexes (Simpson and Kelly, 2012).

Novel Object Recognition (NOR)

The NOR task was performed in a custom made white opaque plexiglass box (40cmx40cmx40cm; City West Plastic, Sydney, NSW). The task was performed as previously described (Bevins and Besheer, 2006) with an inter-trial interval of 24 hours. On day 1, mice were placed into the box and allowed to explore (habituation period) for 5 minutes followed by one hour of rest before the first trial. Two identical non-toxic and odourless objects (cell culture flasks filled with sand) were placed into the box (5cm from each wall) and the mice could explore for 5 minutes. After an inter-trial interval of 24 hours the mice were placed back into the box but one of the old objects was replaced with a new one (tower of Legos blocks) of similar shape, size, and height. The trial ended once a total exploration time of 20 s was reached, or 5 minutes elapsed. A recognition index (RI) was calculated as the time the mouse spent exploring the new object over total object exploration time. Mice were excluded from the analysis if they did not reach the 5-minute exploration criteria. All trials were recorded with an AnyMaze USB camera at 30 frames per second and quantified with a stopwatch by two independent and skilled reviewers.

Barnes Maze (BM)

The Barnes maze task was performed as previously described (Sunyer et al., 2007). An opaque plastic maze was constructed (100 cm in diameter; City West Plastics, Sydney, NSW) with 20 equally-spaced concentric holes around the perimeter. A black

escape box was placed in a random location under one of the holes. Distinct spatial cues (large cut-outs of black shapes – a circle, square, and triangle) were placed on walls around the room and the location of the cues remained constant throughout the testing period. Training on day one consisted of gently guiding the mouse to the escape box and covering it in the dark for one minute. Testing consisted of 4 trials (3 minutes maximum) per day, per mouse, for 4 days in a row. If the mouse could not find the hole after three minutes, it was gently guided there. After each trial completion, the hole was covered in the dark for one minute. All videos were recorded with an AnyMaze USB camera at 30 frames/second and data were analyzed using AnyMaze (Stoelting, Wood Dale, IL, USA) and GraphPad Prism 7. Data are represented as the mean ± SEM in seconds taken to completely enter the escape box from the start of the trial.

QUANTIFICATION AND STATISTICAL ANALYSIS

Statistical parameters, significance, and the exact n (number of animals) values are reported in the figure legends. Metabolic measures, immunoblotting, and behavioral data were separated by sex. Male and female mice were combined for biological replicates in the other analyses because there were no statistically significant differences between sexes. Data were analyzed with Excel, R-studio, and GraphPad Prism 7 (La Jolla, CA, USA). The BM data were analyzed using 2 - way ANOVA (treatment x trial time) with repeated-measures (day) and an ANOVA was used to calculate differences among the groups on individual days. All other data were analyzed by an analysis of variance (ANOVA) with diet treatment as a factor for parametric data followed by a Tukey multiple comparison test with a single pooled variance. For non-parametric data, a Kruskal-Wallis ANOVA was used followed by a Dunn's post hoc multiple comparison test. Linear regression was used to determine relationships between variables and a Pearson's correlation was used to calculate statistically significant relationships. Data are represented as means ± SEM and p values of less than 0.05 were considered statistically significant.

DATA SOFTWARE AND AVAILABILITY

The accession number for the RNA sequencing data reported in this paper is GEO: GSE111778.

Cell Reports, Volume *25*

Supplemental Information

Comparing the Effects of Low-Protein and High-Carbohydrate Diets and Caloric Restriction on Brain Aging in Mice

Devin Wahl, Samantha M. Solon-Biet, Qiao-Ping Wang, Jibran A. Wali, Tamara Pulpitel, Ximonie Clark, David Raubenheimer, Alistair M. Senior, David A. Sinclair, Gregory J. Cooney, Rafael de Cabo, Victoria C. Cogger, Stephen J. Simpson, and David G. Le Couteur

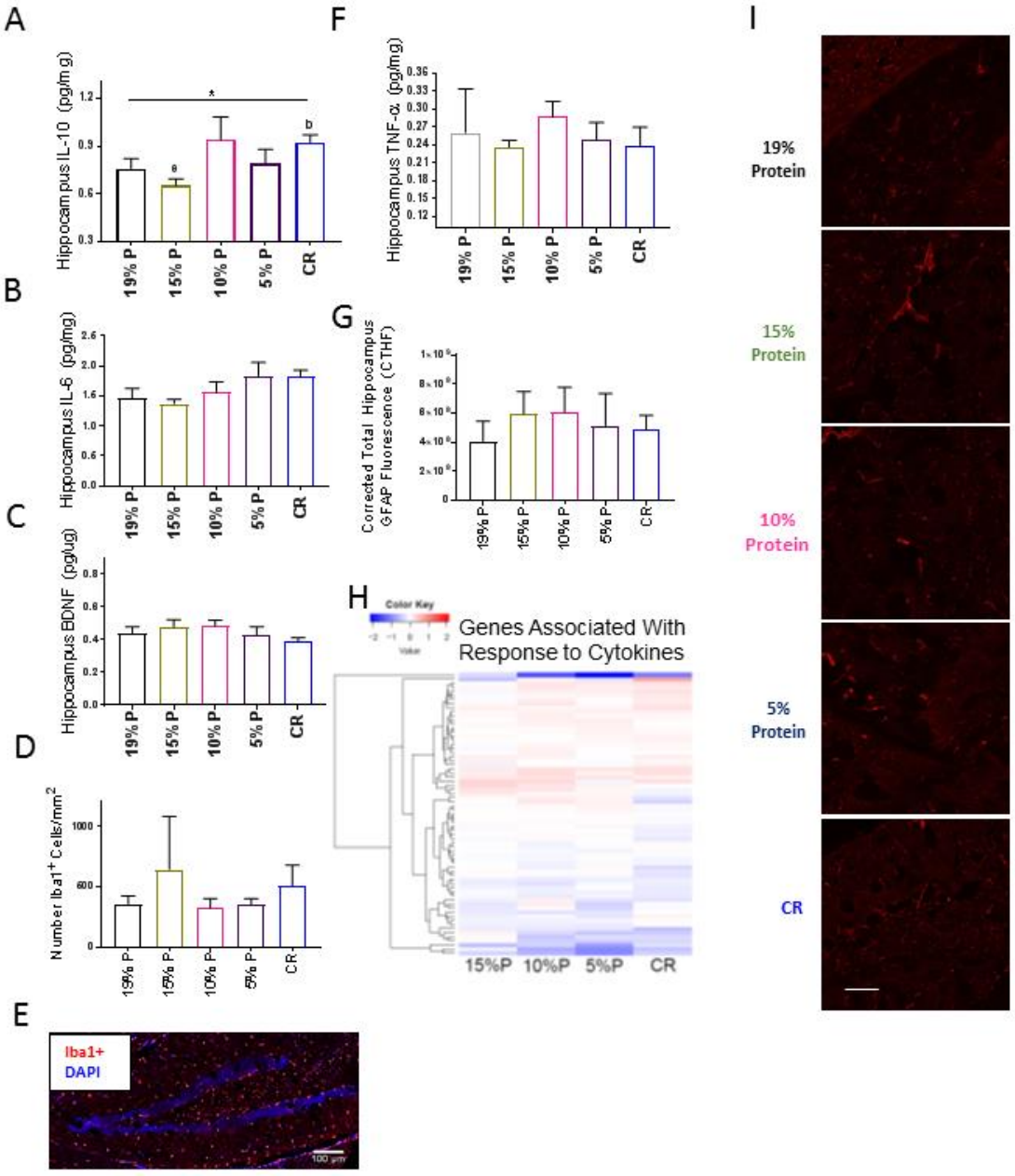

Figure S1. Hippocampal changes in markers of inflammation and associated gene changes in response to CR of LPHC diets, Related to Figure 1.

(A) IL-10 concentrations as measured by ELISA. n=8 biological replicates (4 male, 4 female) per experimental group, 15 months of age. *p < 0.05, **p < 0.01, ***p < 0.001, ****p<0.0001 Kruskal-Wallis ANOVA. a = significantly different to 19% P; b= significantly different to 15% P; c=significantly different to 10% P; d=significantly different to 5% P; e=significantly different to CR as determined by a Dunn's post-hoc analysis.

(B) IL-6 concentrations as measured by ELISA. n=8 biological replicates (4 male, 4 female) per experimental group, 15 months of age.

(C) BDNF concentrations as measured by ELISA. n=8 biological replicates (4 male, 4 female) per experimental group, 15 months of age.
(D) Number of $Iba1^+$ cells per mm^2 of hippocampus and representative image, 15 months of age, n=3-7 biological replicates per experimental group. All data are represented by the mean ±SEM of the biological replicates.
(E) Representative image of Iba1 immunofluorescence staining. Scale bar=100 μm.
(F) TNF-α concentrations as measured by ELISA. n=8 biological replicates (4 male, 4 female) per experimental group, 15 months of age.
(G) Corrected total hippocampus GFAP immunofluorescence in the hippocampus, 15 months of age, 3 – 6 biological replicates per experimental group. All data are represented by the mean ±SEM of the biological replicates. Scale bar = 100 μm.
(H) Heatmap of significantly upregulated or downregulated genes involved to some degree in response to cytokines as revealed by the AmiGO gene ontology online database. Each experimental group is compared to 19% P, and the degree of relatedness among the genes is shown on the y-axis. n=6 biological replicates per experimental group. See also Table S9.
(I) Representative images of GFAP immunofluorescence staining in the hippocampus of each group. Scale bar = 100 μm.

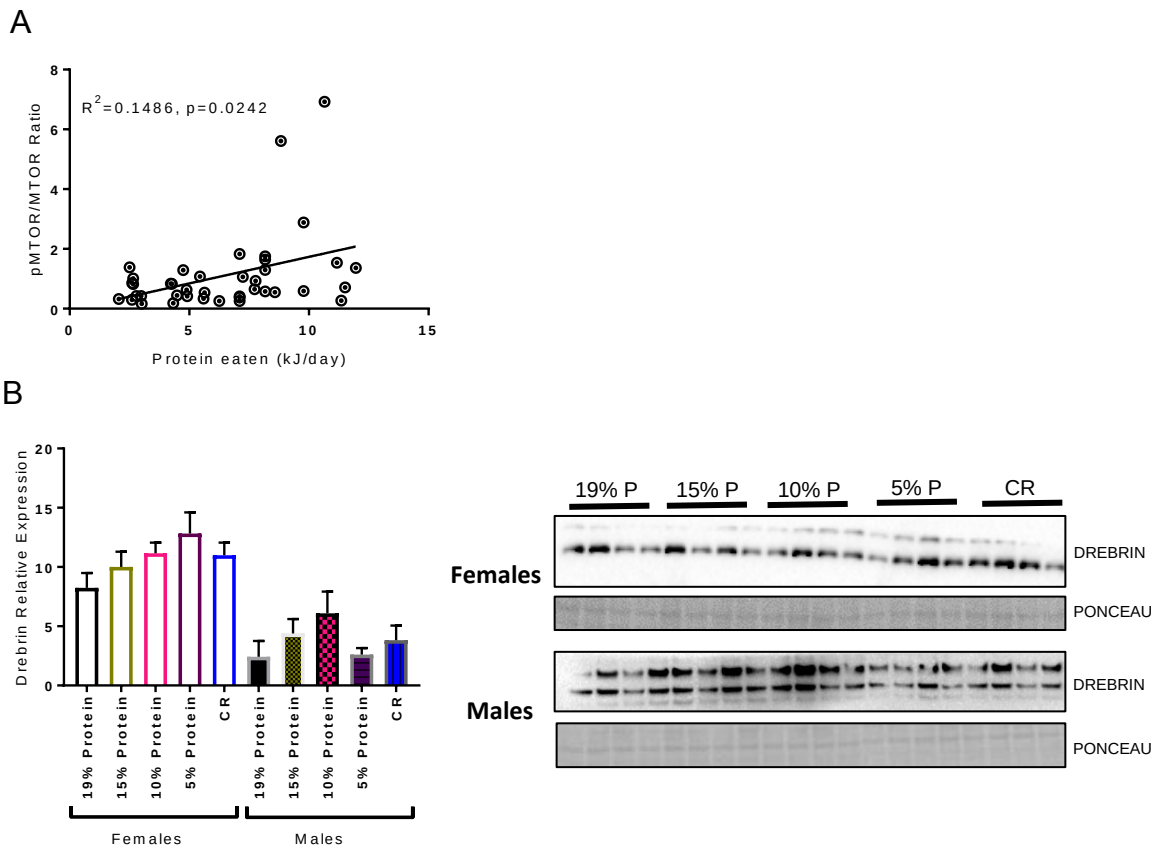

Figure S2. (A) Correlation of average protein intake measured from 12 – 15 months of age and p-mTOR/mTOR as measured by immunoblotting. 15 months of age, 14 months on diet, n=40 (B) Drebrin protein expression as measured by immunoblotting, n=4 mice per experimental group, Related to Figures 2 and 3.

Table S1. Systemic and cardiometabolic measurements related to mouse health and the differences among the groups as determined by ANOVA, Related to Figure 1.

	19% Protein F	**15% Protein F**	**10% Protein F**	**5% Protein F**	**CR F**	
Number of values	12	12	11	12	12	
Urea (mmol/L)	8.13	5.99	4.51	3.12	5.9	****
Std. Error of Mean	0.52	0.37	0.13	0.19	0.29	
	19% Protein M	**15% Protein M**	**10% Protein M**	**5% Protein M**	**CR M**	
Number of values	12	12	12	12	12	
Urea (mmol/L)	7.31	5.64	5.43	3.02	5.88	****
Std. Error of Mean	0.5	0.33	0.29	0.16	0.27	
	19% Protein F	**15% Protein F**	**10% Protein F**	**5% Protein F**	**CR F**	
Number of values	12	11	10	11	11	
Albumin (g/L)	31.67	24.91	27.7	25.45	26.64	p=0.07
Std. Error of Mean	0.86	1.95	2.1	2.57	1.33	
	19% Protein M	**15% Protein M**	**10% Protein M**	**5% Protein M**	**CR M**	
Number of values	12	10	12	12	12	
Albumin (g/L)	30.25	24.9	30.42	27.08	25.17	p=0.06
Std. Error of Mean	0.89	3.31	1.19	1.35	1.49	
	19% Protein F	**15% Protein F**	**10% Protein F**	**5% Protein F**	**CR F**	
Number of values	11	11	9	11	11	
Alanine Transaminase (U/L)	60.45	59.18	77.44	31.91	31.27	**
Std. Error of Mean	12.34	9.375	10.55	8.201	3.063	

	19% Protein M	15% Protein M	10% Protein M	5% Protein M	CR M	
Number of values	12	10	12	12	12	
Alanine Transaminase (U/L)	109.6	100	78.33	61.67	48.08	**n.s**
Std. Error of Mean	20.71	26.43	11.68	35.16	18.18	
	19% Protein F	**15% Protein F**	**10% Protein F**	**5% Protein F**	**CR F**	
Number of values	8	8	8	8	8	
RQ (CO_2 eliminated/O_2 consumed)	0.85	0.86	0.85	0.88	0.85	**n.s**
Std. Error of Mean	0.03	0.02	0.02	0.02	0.02	
	19% Protein M	**15% Protein M**	**10% Protein M**	**5% Protein M**	**CR M**	
Number of values	8	8	8	8	8	
RQ (CO_2 eliminated/O_2 consumed)	0.86	0.78	0.86	0.87	0.88	**n.s**
Std. Error of Mean	0.03	0.07	0.03	0.02	0.01	

Table S2. The top 10 differentially regulated genes when comparing each group to 19% protein as determined by whole-hippocampus RNA sequencing, Related to Figure 2.

CR	log2Fold	padj	5% protein	log2Fold	padj	10% protein	log2Fold	padj	15% protein	log2Fold	padj
Pcmtd1	-0.3	9.63E-08	***Gpr17***	0.45	0.0001624	***Gpr17***	0.55	1.35E-07	***Gpr17***	0.59	4.70E-09
Ogt	-0.22	5.91E-06	***Banp***	0.35110019	0.07741306	***Dpysl5***	0.6	0.000512442	***Hspa5***	0.43	5.43E-05
Mgea5	-0.23	6.65E-06	***Hps4***	0.33538882	0.07741306	***Celf6***	0.48	0.000512442	***Zkscan2***	-0.48	5.43E-05
Dbp	0.66	1.41E-05	***Tbkbp1***	0.27080488	0.07741306	***Gabrb2***	-0.36	0.000512442	***Hif3a***	1.5	7.52E-05
Krit1	-0.28	1.41E-05	***C1qb***	0.25910273	0.07741306	***Hif3a***	1.37	0.000558493	***Hyou1***	0.27	0.00018658
Nr2f6	0.58	4.94E-05	***Adam15***	0.22450936	0.07741306	***Sin3b***	0.27	0.000558493	***Zfp46***	-0.39	0.00018658
Zfp46	0.37	5.15E-05	***Bicd2***	0.20701693	0.07741306	***Htra1***	0.27	0.000558493	***Sdf2l1***	0.65	0.00027147
Dpp8	-0.19	5.15E-05	***Nr1d2***	-0.2183401	0.07741306	***Adam15***	0.28	0.000645404	***Zbtb16***	0.82	0.00032782
Dchs1	0.47	6.31E-05	***Ppm1k***	-0.2571362	0.07741306	***Pik3r3***	-0.32	0.000645404	***Xbp1***	0.36	0.00064116
Cited2	0.53	6.48E-05	***Rab26***	0.33478248	0.08287597	***Sema4b***	0.43	0.000708531	***Plin4***	2.22	0.00067156

Table S3. The top 20 genes positively and negatively correlated with daily protein intake (kJ/day) averaged during 12 – 15 months of age, Related to Figure 2.

Positive Correlation	**pearsonR**	**pearsonP**
Gabrb2	0.784133581	5.79E-06
9330159M07Rik	0.736824362	4.02E-05
Gm26782	0.706759482	0.00011304
Tox	0.696467344	0.00015653
Wwp1	0.695299857	0.00016228
Nr3c1	0.692538917	0.00017662
4930570G19Rik	0.691203312	0.00018395
Kcnj2	0.689924315	0.00019121
Rbms1	0.689492841	0.00019372
Ackr2	0.684763554	0.00022312
Rfc4	0.681916376	0.00024264
Klf7	0.675662426	0.00029079
1190002N15Rik	0.670712936	0.00033458
Abca5	0.670653265	0.00033514
Pou2f1	0.66813019	0.00035963
Gm37893	0.667798783	0.00036296
Ankrd45	0.666294702	0.00037841
Gpr21	0.66539544	0.00038791
Fgf22	0.6609034	0.00043855
Adam22	0.655440583	0.00050778
Negative Correlation	**pearsonR**	**pearsonP**
Zc3h13	-0.7260193	5.92E-05
Tnfsf9	-0.7213022	6.97E-05
Nkd2	-0.7098425	0.00010227
Rasip1	-0.7000014	0.00014018
Sema4f	-0.691355	0.0001831
Scfd2	-0.6886966	0.00019842
Gm12397	-0.6885625	0.00019922
Bicd2	-0.6873154	0.00020681
Tubb2b	-0.6673107	0.00036791
Dchs1	-0.6662718	0.00037865
Sap30	-0.6600511	0.00044878
Chrd	-0.6575432	0.00048009
AI846148	-0.6540868	0.00052632
Syt3	-0.6501643	0.00058342
Tm6sf2	-0.6486166	0.00060737
AI429214	-0.647457	0.00062587
Sin3b	-0.6473848	0.00062704
H2afy	-0.6416336	0.00072632
Cys1	-0.6414134	0.00073037
Pald1	-0.6399919	0.00075703

Table S4. All shared genes between CR and lower protein, higher carbohydrate intake groups, Related to Figure 2.

Shared gene upregulated with CR and overexpressed with lower protein intake (indicated by a negative Pearson correlation)	**CR log2fold Change compared to 19% protein**	**padj**	**pearsonR**	**pearsonP**
sSema4b	0.35405266	0.00395479	-0.4564001	0.02497717
Dll1	0.39680323	0.04350238	-0.4584617	0.02424797
Comtd1	0.43191836	0.03282046	-0.460656	0.02349074
Cpt1c	0.23754724	0.01157335	-0.4608663	0.02341919
Gpc1	0.28894253	0.04392112	-0.4672625	0.02132536
Csf1r	0.27288127	0.0434855	-0.4713588	0.0200659
Caskin1	0.26486868	0.00202484	-0.4716514	0.01997831
Gal3st3	0.3972901	0.00603562	-0.4787775	0.01793871
Samd14	0.50928462	0.0079495	-0.4797691	0.01766886
Nop56	0.19101881	0.01455354	-0.4827977	0.01686502
Tspyl2	0.20810608	0.00687638	-0.4839497	0.01656722
Trim11	0.22123632	0.04413688	-0.4906383	0.01492168
Gm13375	0.64435866	0.00016257	-0.4990689	0.01304064
Hspa2	0.4416678	0.00193604	-0.499491	0.01295185
Tbkbp1	0.28845956	0.00181942	-0.5070009	0.01145318
Gm7367	0.55333569	0.0271947	-0.5116942	0.01059142
Irs2	0.39567919	0.0192398	-0.5123711	0.01047167
Nup214	0.22864657	0.03726844	-0.5149816	0.01002029
Foxo6	0.73404501	0.00828187	-0.5246487	0.00848648
Ap2a2	0.25068819	0.00241388	-0.5321432	0.00743631
Nr2f6	0.57619746	4.94E-05	-0.5367311	0.00684858
Pcdh8	0.59059	0.01599156	-0.5578539	0.00461804
Ebf4	0.34335844	0.01988292	-0.5632839	0.00415579
Cpe	0.19651479	0.0028257	-0.5673905	0.00383267
1700017B05Rik	0.55912801	0.00017238	-0.5676455	0.00381332
Dmwd	0.20250142	0.00301955	-0.5689788	0.00371352
Icam5	0.35340368	0.01668618	-0.5703367	0.00361414
Wscd1	0.29228139	0.00395479	-0.57126	0.00354786
Fbxo21	0.22978884	0.00301955	-0.5771505	0.00314871
2510039O18Rik	0.29879598	0.00121498	-0.5787825	0.0030451
Bcar1	0.18898261	0.0492433	-0.5892797	0.00244525
Kcng2	0.68077627	0.02018061	-0.5944876	0.00218705
Prkcsh	0.16888627	0.01603777	-0.5965451	0.00209164
Prdm8	0.44193864	0.04848226	-0.604109	0.00177072
Grasp	0.28017977	0.02323257	-0.6107547	0.00152441
Aldoa	0.20282323	0.00208295	-0.6107806	0.00152351

Adam11	0.25321804	0.04350238	-0.6317069	0.0009297
Sin3b	0.18626064	0.01860923	-0.6473848	0.00062704
Syt3	0.25567563	0.00422911	-0.6501643	0.00058342
Dchs1	0.46948691	6.31E-05	-0.6662718	0.00037865
Shared gene downregulated in CR and under expressed with lower protein intake (indicated by a positive Pearson correlation).	**CR log2fold Change compared to 19% protein**	**padj**	**pearsonR**	**pearsonP**
Gabrb2	-0.3508222	0.00018875	0.78413358	0.00000579
Klf7	-0.2217289	0.03548333	0.67566243	0.00029079
Ankrd45	-0.3521763	0.00123508	0.6662947	0.00037841
Gabra1	-0.310818	0.04736295	0.63382655	0.00088259
Kcnh7	-0.6226457	0.03486339	0.6330891	0.00089874
Ptpn4	-0.3417165	0.00235884	0.61488654	0.00138655
Ppm1k	-0.2359459	0.01519108	0.61390032	0.00141845
Il1rapl1	-0.3754498	0.04413688	0.60033979	0.00192494
Kcnh5	-0.9108005	0.03642204	0.59523422	0.00215201
Pik3r3	-0.2398985	0.0081861	0.59402245	0.00220912
Tab3	-0.2474935	0.00681953	0.59386447	0.00221666
Pgr	-0.4488183	0.01157335	0.58760374	0.00253367
Zfyve9	-0.2056544	0.00470079	0.58703924	0.00256405
Fbxl3	-0.125008	0.0492433	0.58524524	0.00266268
Pde7b	-0.7022167	0.01988292	0.57891453	0.00303685
Trim37	-0.2730551	0.00808642	0.57806273	0.00309043
Abcd2	-0.4812836	0.01830501	0.56309238	0.00417141
Cacnb4	-0.404557	0.04698135	0.55710299	0.00468523
Ccng1	-0.3696455	0.00076862	0.55567729	0.00481509
Ptar1	-0.4602855	0.00321787	0.54848416	0.00551729
Plag1	-0.4717523	0.01772261	0.54474836	0.0059146
Nxt2	-0.2335756	0.0271947	0.54411182	0.00598463
Zfp106	-0.1500603	0.00016078	0.54147036	0.00628269
Pvalb	-0.5989511	0.02198946	0.53723473	0.0067865
Spcs3	-0.2220862	0.04736295	0.53280558	0.00734894
Spag9	-0.1668287	0.00029442	0.52601692	0.00828607
Atrnl1	-0.3261077	0.0286946	0.52594548	0.00829644
Tmem56	-0.3539449	0.01730313	0.52466698	0.00848378
Tmem14a	-0.3502767	0.04223044	0.52126277	0.0089998
Gprin3	-0.5619832	0.02821759	0.49492424	0.01393944
Cdh12	-0.5120774	0.01988292	0.48018983	0.01755535
Rgs7bp	-0.2796904	0.00192408	0.47954087	0.01773067
Creb1	-0.1782215	0.0167314	0.47816274	0.01810769
Klf6	-0.2859272	0.02748043	0.46765283	0.02120265

Table S6. The log2fold values of each gene involved in *mus-musculus* anti-aging when comparing each group to 19%P as revealed by *GenAge*, the online aging gene database, Related to Figure 2.

Anti-longevity	**15% protein**	**10% protein**	**5% protein**	**CR**
Adcy5	0.00101141	0.05771784	-0.0523274	-0.0534537
Cdkn1a	0.7377191	0.35277723	0.54534961	-0.7218583
Coq7	-0.0737427	0.00790468	-0.1330624	0.04306016
Ghr	-0.0975083	-0.0622679	-0.1283798	-0.0774089
Gpx4	-0.0120894	0.02557822	-0.0212931	0.03566496
Igf1r	0.10137465	-0.0513397	-0.0435251	-0.0809981
Insr	-0.0826957	-0.0620446	-0.1249071	0.00858514
Irs1	0.01163419	-0.0842415	-0.0278227	0.1763891
Irs2	0.415006	0.38797032	0.33342455	0.39567919
Pappa	0.12777558	0.14983361	0.06923623	0.32701302
Shc1	-0.0085756	0.05193752	-0.1203029	0.05694044
Surf1	-0.041281	0.0327547	-0.0322512	0.03530401
Terf2	0.01977974	-0.0201558	-0.0127406	0.05504929
Agtr1a	0.29542411	0.40157403	-0.0768968	0.6068944
Eef1e1	0.10322327	0.00036954	0.10715376	0.02357882
Eps8	0.22462836	0.20697937	0.11479969	0.07668302
Htt	0.0247453	-0.0075698	0.05237501	0.00793609
Kcna3	-0.0507403	0.01600972	0.02044149	-0.0960018
Trp53bp1	0.08334146	0.08299112	0.04582947	0.04969909
Rps6kb1	-0.0358813	-0.1126248	0.01474385	0.01180968
Prkar2b	-0.066228	-0.1862829	-0.1960429	-0.229938
Eif5a2	-0.105278	-0.1477355	-0.0895156	-0.2019709
Mif	0.03320796	0.04232219	-0.0038491	0.06173697
Dgat1	0.02517592	0.17927008	0.08849546	0.21041512
Gsta4	-0.0276925	0.04205657	-0.0100078	0.02963213
Mtor	0.07834324	0.0802618	0.05700023	0.13390206
Akt1	-0.0098096	0.03854792	0.0135716	0.04650128
Ikbkb	0.01562326	0.02150382	0.08282916	-0.0622174
Serpine1	0.56801856	0.45845617	0.11176432	0.38427494
Myc	0.35789686	0.37327365	0.26443569	0.34441771
Ctf1	0.04690428	0.18322558	-0.0154515	0.60451893
Trpv1	-0.8993551	0.33012914	-0.3504407	-0.2146092
Adra1b	-0.1498984	-0.648872	-0.5868867	-0.5445847
Mtbp	-0.1725916	0.00078446	-0.1709641	0.03955118
GMFB	-0.0162379	-0.0598283	0.04766998	-0.1754922
Per2	0.30984155	0.2393255	0.22066461	0.16328089

Table S7. The log2fold values of each gene involved in *mus-musculus* pro-aging when comparing each group to 19%P as revealed by *GenAge*, the online aging gene database, Related to Figure 2.

Pro-longevity	**15% protein**	**10% protein**	**5% protein**	**CR**
Arhgap1	0.01472539	0.02169014	0.0283409	0.04870202
Arntl	-0.0235492	-0.0922206	-0.0117955	-0.296538
Atm	-0.1350654	-0.1323911	-0.0631488	-0.1103872
Atr	-0.157324	-0.1734812	-0.1028854	-0.1585894
Brca1	-0.1799138	-0.4354884	0.0697703	-0.2901321
Bub1b	-0.5832571	-0.2441502	0.17637462	-0.1148866
Bub3	-0.0140228	-0.0550891	-0.0429496	-0.0357142
Casp2	-0.2311755	-0.034555	-0.0794455	0.04008864
Cat	-0.0019598	-0.044525	-0.046639	0.06908542
Cav1	-0.0506545	0.03932483	0.02036309	-0.1862541
Chek2	0.3034059	0.14290546	0.2064488	0.22604372
Efemp1	-0.0010094	0.12383775	-0.299932	-0.0501378
Ercc2	0.11967058	0.21557756	0.09748366	0.23052638
Ercc4	0.01829984	-0.0393227	0.03393852	0.04402606
Foxm1	0.39617119	0.3546454	0.41792158	0.26177433
Fxn	0.30521288	0.40300464	0.30338086	0.21960896
Hells	-0.0551892	-0.4533302	-0.2362269	-0.2805961
Htr1b	0.11440774	-0.1981081	-0.2953036	-0.3121809
Kl	-0.1645951	-0.724464	-1.2783803	-0.1869482
Mcm2	-0.1288324	-0.0379488	-0.0364486	0.17960689
Mgat5	0.05205893	-0.0962008	-0.0287829	-0.0610701
Msh2	-0.184829	-0.1546783	-0.1923001	-0.2006773
Msra	-0.1441285	0.00817381	-0.0222092	0.07818727
Neil1	-0.0442839	0.06125585	0.05353876	-0.0482191
Nos3	0.09270389	0.16102161	0.07008146	-0.0127572
Pawr	0.48891806	0.30262196	0.12309857	0.30313031
Plau	0.12046579	-0.1699962	-0.2446204	-0.146323
Polg	-0.0507667	-0.0414472	-0.0575781	0.00198663
Ppm1d	-0.0921606	-0.066257	-0.1730867	0.06070633
Prdx1	-0.0632609	-0.1009401	-0.0722758	-0.0465243
Rae1	-0.0646415	0.05941629	0.04225784	0.15557218
Sirt6	0.0747384	0.10655685	0.08336311	0.1374625
Slc25a4	-0.0493511	-0.0492517	-0.0291346	-0.0188985
Stub1	0.04627869	0.05517608	0.05667367	0.08146132
Tert	-0.220479	0.09297109	0.19679318	-0.1721455
Top3b	-0.0132511	-0.0420395	0.00995746	0.04664054
Trp53	-0.1050617	0.02056071	-0.0228488	0.14547218

Trp63	-0.0237196	-0.0220774	-0.159791	-0.4238329
Txn1	-0.1197964	0.0342771	0.0503297	-0.0382848
Ucp2	0.22380362	0.16068458	-0.1717167	0.24193137
Xpa	-0.2123533	-0.1424581	0.00965685	-0.0536911
Xrcc5	0.04207824	-0.1571704	-0.1187839	-0.0298264
Xrcc6	-0.1114411	-0.1234526	-0.1345597	-0.0366144
Zmpste24	0.01297913	-0.0204502	-0.0648816	-0.1187497
Apoe	0.1288558	0.23588882	0.06155151	0.23889281
Cisd2	-0.0575493	-0.1531616	-0.068797	-0.1075128
Clock	-0.0254955	-0.1162018	-0.0642864	-0.2036687
Dmd	-0.1094382	-0.1136045	-0.0881478	-0.1333848
Fn1	0.07591546	0.34096519	0.0811186	0.16981677
Hnrnpd	0.00353037	-0.0079354	-0.019962	0.03498714
Jund	0.25449322	0.39133029	0.21424433	0.41596706
Pparg	-0.2879742	-0.6457382	-0.3525091	-0.6113942
Sirt7	0.0655924	0.20156253	0.09263095	0.11525205
Socs2	0.00789526	0.11893311	0.14228172	0.01562922
Sod2	0.00589075	-0.0768286	-0.0098854	-0.1439157
Topors	-0.0865081	-0.15807	-0.1448736	-0.0843207
Tpp2	-0.0242168	-0.0684694	0.02095572	-0.0437661
Parp1	0.02931385	0.08868345	0.15697886	0.0770911
Sirt1	0.02226846	-0.1053712	-0.0144651	0.06436107
Pten	0.00963482	-0.1002418	-0.0707925	-0.0758108
Cdc14b	-0.0121771	-0.227941	-0.2742356	-0.2442611
Mt1	0.04160547	0.15355501	0.05442407	0.13364061
Trp73	0.28424114	-0.1068311	-0.4463664	0.27153949
Htra2	-0.0664208	-0.0143931	-0.031976	0.02341684
Gsk3a	-0.0090046	-0.037634	0.0007846	0.02773572
NUDT1	0.12563543	0.1936328	0.00911153	-0.1758967
Sqstm1	0.00416845	0.03353688	0.02217693	0.11893822
Cdk7	-0.0619699	-0.1046035	-0.0776116	-0.0936238
Grn	-0.0116829	0.11031105	0.03003236	0.11047344
Ncor2	0.21859183	0.17958035	0.14104844	0.16339809
Ercc1	0.01312657	-0.0136704	0.06253632	-0.0139188
Rictor	-0.0395646	-0.0869194	-0.0081099	-0.1273791
Atg5	-0.062396	-0.0215193	-0.0368581	-0.0897468
Adra1a	0.02744343	-0.0380839	0.02020799	-0.1409094
Nfkb1	0.07013187	0.07207794	0.09139244	0.06806671
Rbm38	0.20968059	0.23496542	0.2971683	0.64836596
Col1a1	-0.1680529	0.13717079	-0.6490787	0.08997952
Siglece	-0.4827507	-0.4301152	-0.2071509	-0.3080146
SOD3	0.10686177	0.18017767	-0.0393098	0.07608005

Table S8. Genes associated with CR and the corresponding log2fold values when comparing each group to 19%P, Related to Figure 3.

Overexpressed with CR	**15% protein**	**10% protein**	**5% protein**	**CR**
Acot12	-0.4510922	-0.0282806	0.09478237	0.15608275
Inmt	-0.4455502	-0.3770715	-0.287243	0.71539539
Mat1a	-0.3018161	-1.3844592	-0.5723038	-0.2298032
Tmem218	-0.2754751	-0.3216527	-0.3111763	-0.3017594
Klf10	-0.2689117	-0.235222	-0.0516133	0.01296802
Epb4.1	-0.2574814	-0.3401682	-0.2811228	-0.2815561
Dbp	-0.2161203	-0.1110509	-0.3084841	0.65835636
Gpr146	-0.2093064	-0.1425984	-0.1245682	-0.0451288
Aldh1a1	-0.2072118	-0.3537867	-0.1784337	-0.2910412
St3gal5	-0.2047768	-0.2017289	-0.0694903	-0.1745451
Sun2	-0.1815075	-0.1281606	-0.1103428	-0.0930545
Rhobtb1	-0.1795693	-0.0471919	-0.0988085	-0.0753131
Mgp	-0.1453807	0.14646765	-0.4430167	0.11290186
Ehhadh	-0.141166	-0.2217855	-0.0391253	0.2352127
Bnip3	-0.1386123	-0.1119989	0.03939532	-0.0804203
Igfbp2	-0.1231492	-0.3704185	-1.0580601	-0.1243689
Usp2	-0.1208957	-0.1807186	-0.2043066	0.12193633
Cyp2j6	-0.1093863	-0.1228871	-0.1889964	-0.0842898
Dusp1	-0.0902481	-0.1788821	-0.3117596	-0.0070359
Ntf3	-0.0834746	0.06064372	0.05948092	0.32655401
Hacl1	-0.083386	-0.2291783	-0.0286324	0.03363977
Ppara	-0.0689816	0.05138249	0.09588951	0.10866857
Slc37a4	-0.0641777	0.04351523	0.0249397	0.04270592
Adcy1	-0.0570892	-0.1947714	-0.029705	-0.1771128
Decr2	-0.0509821	0.02704746	-0.0543016	-0.0726938
Decr1	-0.0508268	-0.1072088	-0.1334743	-0.1762638
Tob1	-0.044159	-0.1874523	-0.2183286	0.07368644
Cbr1	-0.0408525	0.04875346	0.02661066	0.0731318
Per1	-0.0224094	-0.0334725	-0.0285945	0.22766577
Wee1	-0.0216056	-0.0744612	-0.1935011	-0.2043732
Acot4	-0.009239	0.22999321	0.13312325	-0.0117283
Cpt1a	-0.0087565	-0.0543521	-0.2633878	0.1174669
Lpin1	-0.0079843	0.05961562	-0.0030391	0.04540081
Pla2g12a	0.00973676	-0.0053818	-0.022337	0.05238588
Ablim3	0.02178646	-0.0781005	-0.0303703	0.02870046
Rhbdd2	0.02956889	0.04586255	0.00088878	0.03823837
Klf9	0.04064265	-0.0255918	-0.0227936	-0.1127542
Klf9	0.04064265	-0.0255918	-0.0227936	-0.1127542

Mt1	0.04160547	0.15355501	0.05442407	0.13364061
Ifrd1	0.04205248	0.01948604	0.03144177	-0.0418738
Crym	0.04682847	0.37502488	0.35962182	0.31178074
Slc25a25	0.04813346	0.03294377	-0.0181616	-0.0818371
Zfp354a	0.0647907	-0.1386225	0.24452415	0.00846424
Enpep	0.07847471	-0.1889923	-0.1513999	-0.4677518
Nfkbia	0.09375226	0.43106597	0.15339755	-0.0178166
Por	0.10008187	0.06311304	-0.0043761	0.21481561
Sall1	0.11153679	0.025667	-0.0045194	0.14597973
Slc25a42	0.11350385	0.11584435	0.19290471	0.02084894
Fam195a	0.11976624	0.1781308	0.21054772	0.0635081
Pim3	0.13951806	0.2070903	0.09276525	0.16127446
Mt2	0.14890754	0.2766307	0.17300344	0.1476554
Cobll1	0.14983442	0.00249694	0.00184324	0.18703689
Plcxd3	0.15690057	0.10954026	0.121864	-0.090086
Fam107a	0.17038021	0.15551367	0.01805516	-0.2562289
Ctgf	0.17194899	0.24490704	0.17929895	-0.016758
Nat8	0.19793868	0.0250599	-0.1664148	-0.0016687
Cry1	0.20938696	0.02570787	0.01403533	0.06276243
Herpud1	0.26219829	0.04185022	0.07672109	0.05425907
Trp53i13	0.26322852	0.37215079	0.1450828	0.39032931
Smoc1	0.29468753	0.34363698	0.02806185	0.27279036
Per2	0.30984155	0.2393255	0.22066461	0.16328089
Fkbp5	0.33165152	0.31806022	0.30150165	0.09886719
Klf15	0.33594585	0.34486323	0.17454914	0.05100368
Tsc22d3	0.35975863	0.39717674	0.12507946	-0.0896571
Arrdc2	0.38448986	0.39440052	0.29753779	-0.177259
Fzd1	0.39085794	0.44413288	0.13652337	0.55863088
Irs2	0.415006	0.38797032	0.33342455	0.39567919
Sult1a1	0.42825862	0.46386113	0.07635109	-0.0791534
Rgs16	0.43144714	-0.3308686	-0.300976	-0.1803528
Angptl4	0.49113968	0.73679064	0.27201196	0.15678084
Cd163	0.52539695	0.51771548	-0.4282355	-0.1997675
Map3k6	0.56449422	0.58182212	0.39503114	0.16610049
Gys2	0.70771346	-0.2968843	0.63632324	1.52193882
Zbtb16	0.81555612	0.6481624	0.46377654	0.20752908
Plin5	1.11831391	0.29213504	0.18592859	0.81500252
Plin4	2.21956688	1.38281782	1.0719565	0.69817751
Underexpressed with CR	**15% protein**	**10% protein**	**5% protein**	**CR**
Casc5	-1.1915579	-0.9115165	-0.3733886	-0.4002452
Ifi27l2a	-1.0223006	-0.3363049	-1.1486906	0.15412521
Phf19	-0.8146298	-0.2609268	-0.2056072	-0.4251833

Tnfsf10	-0.6984303	-0.4869579	-0.0826616	-0.2735283
Ifih1	-0.5987212	-0.4574485	-0.6186532	-0.4272112
Tmem132d	-0.3745109	-0.4973567	-0.4804528	-0.5382282
Alas2	-0.3558136	-0.257527	-0.0886628	0.54501254
Insig1	-0.342859	-0.3188008	-0.2644325	-0.0074479
Gck	-0.2855682	-0.1010476	-0.1877749	0.53371548
Col15a1	-0.2471893	-0.2388577	-0.2817814	-0.0562077
C4bp	-0.1898903	-0.9261569	0.28982861	0.61588131
Irf7	-0.1737809	-0.0369168	-0.3389087	-0.0266234
Irgm1	-0.1620699	-0.2569813	-0.0610272	-0.1470485
Scrt1	-0.1618382	-0.2410631	-0.2066196	-0.1956099
Extl1	-0.1421953	-0.1540141	-0.056344	-0.0396413
Sc5d	-0.1219082	-0.0894164	-0.057975	-0.1168206
Cdc42ep2	-0.1177925	-0.2260356	-0.0870679	0.13019473
G6pdx	-0.1095388	-0.0764554	-0.1118923	-0.0250055
Ghr	-0.0975083	-0.0622679	-0.1283798	-0.0774089
Slc6a6	-0.0931028	-0.0806533	-0.0540442	0.09558094
Zfp64	-0.0785603	0.00598083	0.0294814	0.11536721
Ly6e	-0.0646478	-0.0214757	0.0685652	-0.0744331
Nr1d1	-0.0329025	-0.106986	-0.2160847	0.45646414
Srebf1	-0.0257264	0.12923937	-0.0652295	0.3449339
Fabp5	-0.0254908	0.00881646	-0.01323	0.06591191
Arntl	-0.0235492	-0.0922206	-0.0117955	-0.296538
1110051M20Rik	-0.0068467	0.05837647	0.05276045	0.02034748
Dhcr7	-0.0062799	-0.0128339	0.0843046	-0.0362128
Acly	-0.002286	-0.016171	-0.0683946	-0.0665175
Psmb8	0.00410806	-0.0244623	0.08102317	-0.0097197
Scly	0.01006253	-0.0055203	-0.106322	-0.0494183
R3hdm2	0.02121147	-0.1549211	-0.0949987	-0.2178529
Gtf2ird1	0.02962381	-0.0835866	-0.0947068	0.08469086
Litaf	0.05273628	-0.0769627	-0.0290641	0.12214575
Dpp9	0.08204702	0.06567618	0.07891555	-0.0107709
Stac3	0.08858554	-0.0270473	0.11122527	0.13789108
Actg1	0.10932333	0.17951554	0.08617046	0.34357994
Pdia3	0.13168417	0.03701201	0.01424799	-0.1994026
Ptprj	0.13291944	-0.0315285	0.06656098	-0.0084613
G0s2	0.14072088	0.17985659	0.30948104	0.13054967
Hipk2	0.14756454	0.00044062	-0.0055519	-0.1040742
Phlda1	0.16046551	-0.019217	-0.0082457	0.10433809
Serpinh1	0.16663189	0.10050277	-0.1119897	-0.0313443
Cldn1	0.18630663	-0.5353095	-0.8608371	-0.0642067
Mmp15	0.19812773	0.12577564	-0.0740732	-0.0370251

Ttll12	0.22451206	0.18176083	0.1011936	0.15092252
Dnase1l2	0.2358725	0.24456262	0.25622468	-0.0177012
Hspa5	0.43436974	0.20979303	0.15726423	-0.2931173

Table S9. The top differentially genes associated with cytokine response as determined by and the corresponding log2fold values when comparing each group to 19%P, Related to Figure 1.

GO:0034097: Response to cytokine	**15% protein**	**10% protein**	**5% protein**	**CR**
Prlr	-0.3124379	-1.4854024	-2.1264179	-1.0987817
Il2ra	-0.5127679	0.09017402	-0.2243204	0.76074868
Lepr	-0.380699	-0.6124417	-0.9759275	-0.380013
Il20ra	-0.5622562	-0.3511454	-0.8281828	-0.2487755
Socs1	0.08811141	-0.3144046	-0.4770619	-0.4164325
Tnfrsf11a	0.0362551	-0.4523289	-0.266672	-0.2844594
Sigirr	-0.1517293	-0.1743266	-0.1923981	-0.5195826
Grem2	0.03539414	0.14672447	0.08904538	-0.2392744
Mkks	-0.0148601	-0.1399518	0.06324986	-0.3196247
Stat6	-0.0483035	-0.3804103	-0.3950694	-0.3218779
Parp9	-0.1261586	0.12127626	-0.2192537	-0.2226355
Irf7	-0.1737809	-0.0369168	-0.3389087	-0.0266234
Irf3	0.21830031	0.21247326	0.06261317	-0.0830612
Adipor2	0.34075238	0.20656695	0.10639012	0.00965924
Il10rb	-0.1297183	-0.063788	-0.2116667	0.09160023
Ripk2	-0.1681861	-0.2638534	-0.2004819	0.00583
Ptpn2	0.19040233	0.0610843	0.06838353	-0.0904268
Tnip2	-0.0517848	0.13181735	0.11696048	0.22270761
Jak2	0.03915672	-0.0240166	0.01805368	-0.1995238
Tnfrsf1a	0.05299786	0.20940839	-0.017096	0.17760221
Trp53	-0.1050617	0.02056071	-0.0228488	0.14547218
Cav1	-0.0506545	0.03932483	0.02036309	-0.1862541
Parp14	-0.0112184	-0.0505822	-0.0618727	-0.2309541
Slc27a1	0.16101155	0.29478276	0.09296984	0.25022265
Ptk2b	-0.0263274	0.0623601	0.09468539	0.18805537
Nol3	-0.0294703	0.12527003	0.03103341	0.15922547
Pias4	0.12979144	0.06255174	0.08790193	0.25625004
Kit	0.03252986	0.18885826	0.17344145	0.22149999
Acsl1	-0.1222602	-0.1462795	-0.1658713	0.0163453
Irgm1	-0.1620699	-0.2569813	-0.0610272	-0.1470485
Peli3	-0.0567931	0.11092357	-0.0281605	0.0637812
Sirt1	0.02226846	-0.1053712	-0.0144651	0.06436107
Stat2	-0.042218	-0.0124125	0.07106699	-0.1024895
Gab1	0.12752407	0.10163881	-0.0151442	0.14445643
Fer	-0.0972999	-0.1281971	-0.0033358	-0.1728492
Il1r1	-0.0206728	0.03637892	0.10896669	-0.0483269
Tjp2	0.12938579	0.00751226	-0.028789	0.06469961

Flt3	-0.0569778	-0.1759885	-0.0786975	-0.1942215
Cx3cr1	0.00476811	0.12471401	0.15210297	0.04912149
Jagn1	0.0095568	0.04512287	-0.0216618	-0.1091516
Bbs4	-0.0249573	-0.0140786	0.00858946	-0.1366441
Traf3	0.1727386	0.22543352	0.24589551	0.10329988
Mt3	0.05115107	0.10850541	0.12232796	-0.0133889
Stat1	0.00326868	0.12226689	0.00690766	-0.0089325
Ikbkb	0.01562326	0.02150382	0.08282916	-0.0622174
Cib1	0.07730703	0.20710862	0.12418305	0.1798827
Otulin	-0.0037782	-0.0922348	-0.0454188	0.03129271
Trim32	0.00896249	0.01671982	0.05668749	0.11179068
Traf6	0.061785	-0.0056239	0.05390657	0.10552657
Irf1	-0.030716	0.07553137	0.03442714	0.05023534
Adar	0.04747298	0.03806305	-0.0098541	-0.0495348
Fkbp1a	-0.003495	0.03866164	0.10328484	0.06589078
Crebrf	-0.0458969	-0.1190454	-0.1163381	-0.1505748
Csf1r	0.18230967	0.26893674	0.22037066	0.27288127
Stat3	0.04760643	0.13692599	0.04511536	0.06878485
Bbs2	-0.038754	-0.0809681	0.02165674	-0.0313752
Adipor1	-0.009471	-0.0388892	-0.0997059	-0.0173026
Cx3cl1	-0.0159395	-0.1087117	-0.0386722	-0.0736198
Ifnar1	-0.0897248	-0.1162311	-0.0788426	-0.0319161
Rabgef1	-0.016632	-0.067883	-0.0263551	-0.0846645
Zcchc11	-0.1418487	-0.1923305	-0.1438413	-0.1178958
Sharpin	0.05408174	0.10035881	0.12055046	0.11199024
Il1rap	0.04642549	0.04047231	0.10001194	0.04719802
Ctr9	0.00306432	0.01857674	0.0185325	-0.0401354
Med1	0.03173762	-0.0023999	0.0292154	-0.0215872

Table S10. The top differentiated genes associated with dendrite morphogenesis and the corresponding log2fold values when comparing each group to 19% protein, Related to Figure 4.

GO:0048813: Dendrite morphogenesis	**15% protein**	**10% protein**	**5% protein**	**CR**
Cacna1f	-0.0183999	-0.3600848	-0.5399677	0.37805278
Sema3a	-0.1114775	-0.9538858	-0.5631468	-0.8613153
Xlr3b	0.37932445	-0.0122672	0.20431643	-0.304775
Nfatc4	-0.3097113	-0.0687018	-0.3471485	0.14849524
Ephb3	-0.3315877	-0.3066718	-0.0838266	0.14847308
Atp7a	0.06392776	-0.1854235	-0.2475899	-0.3367102
Cux2	-0.1512067	-0.5112572	-0.4520998	-0.4175882
Chrna7	-0.1929339	0.02888425	0.1099817	0.03311738
Cux1	-0.1900122	-0.4923989	-0.3885139	-0.3632077
Ephb1	0.04139052	-0.1638925	0.01568811	0.08827617
Zfp365	-0.0917968	-0.176813	-0.0257962	-0.270881
Dact1	0.00614278	0.0783615	-0.0075147	0.21958902
Cdkl3	-0.1659417	-0.1299049	-0.0340576	0.06355596
Caprin2	-0.1937324	0.00236138	-0.0325774	-0.0271619
Prex2	0.08877366	0.04804348	0.03671918	-0.1112024
Epha4	-0.1314543	-0.0892548	0.05932841	0.00579808
Nlgn3	0.13263807	0.06230024	0.0891848	0.24459838
Ptprd	-0.037442	-0.1844852	-0.0924727	-0.2093489
Rbfox2	0.06520249	0.04149948	0.03738559	-0.1095126
Kalrn	-0.1863182	-0.2214488	-0.0915808	-0.0617582
Il1rapl1	-0.2054591	-0.3204012	-0.2665911	-0.3754498
Slc11a2	-0.0974959	0.00430504	0.00288069	0.07924403
Slitrk5	-0.0916813	-0.0835903	-0.0174982	0.06277435
Ankrd27	-0.0923923	-0.0315642	0.07105617	0.02286226
Elavl4	-0.0840633	-0.2331131	-0.1408282	-0.2119659
Ephb2	0.15298138	0.13131575	0.1707556	0.28418091
Arhgap44	-0.0158529	-0.0929735	-0.007467	0.07149749
Caprin1	0.03663942	0.0020223	0.01197248	-0.1106857
Dock10	0.26257051	0.12765267	0.14990567	0.13176725
Ppp3ca	-0.1477279	-0.1695103	-0.0473339	-0.0518907
Ss18l1	-0.032182	-0.0450651	0.02646264	0.0929691
Vldlr	-0.0603936	-0.0627664	-0.0572817	0.06552959
Pak3	0.08804301	0.04058181	0.0644234	-0.0540939
Fmn1	-0.2406328	-0.3392874	-0.1949128	-0.2751251
Nlgn1	-0.0935203	-0.0840151	0.03405325	-0.0277452
Rab21	0.0510943	-0.0577027	0.00156715	-0.0706992
Reln	0.20969432	0.27236936	0.14353411	0.18055388

Lrp8	0.06803703	0.10847874	0.10751869	-0.005584
Camk2a	0.01643545	0.06209554	0.1198379	0.13090484
Mapk8	-0.065824	-0.1015729	-0.0046997	-0.1267613
Itgb1	0.00413143	-0.0857656	-0.1152058	-0.0955679
Dscam	-0.0637295	-0.0532056	-0.0829103	0.03477883
Pten	0.00963482	-0.1002418	-0.0707925	-0.0758108
Dtnbp1	-0.0845296	-0.0844208	0.00741362	-0.0278588
Picalm	0.0466801	-0.0161881	0.03264976	-0.0508746
Mapk8ip2	0.04528685	0.09765425	0.06541195	0.14744807
Fyn	0.0098059	0.08234397	0.10107542	0.08454398
Cdk5r1	-0.0209863	-0.0693114	-0.0540815	0.02016562
Hprt	-0.1327103	-0.150682	-0.0644663	-0.1115482
Kidins220	-0.0144046	-0.0188056	-0.0079433	-0.0871573
Pafah1b1	-0.0839754	-0.1043807	-0.0177611	-0.0683855
Hdac6	0.05399071	0.11111336	0.08960867	0.13716647
Abl2	0.0728928	0.07181999	0.08803355	0.01756956
Dvl1	0.08825457	0.08302734	0.08207024	0.0257026
Cdk5	-0.032159	0.02545157	0.02843784	-0.0105184
Rere	0.15253974	0.171391	0.11536209	0.11597048
Ctnna2	-0.0800337	-0.121171	-0.0583412	-0.0964205
Wasl	0.06028392	0.00485558	0.04359949	0.04627474
Rapgef2	0.08429412	0.10281787	0.09172912	0.13554566
Cacna1a	-0.0363766	-0.0801176	-0.0436606	-0.0391737
Shank3	0.11053102	0.14201556	0.1398349	0.1051724
Cdc42	-0.0917285	-0.0933177	-0.0686672	-0.0744869
Klf7	-0.2077166	-0.2206282	-0.223446	-0.2217289